954 506

(ERDA/JPL-954506-78/1)   HOT FORMING OF   N78-28600
SILICON SHEET, SILICON SHEET GROWTH
DEVELOPMENT FOR THE LARGE AREA SILICON SHEET
TASK OF THE LOW COST SILICON SOLAR ARRAY   Unclas
PROJECT   Final Report, 12 May (Pennsylvania   G3/44   25942

HOT FORMING OF SILICON SHEET, SILICON SHEET GROWTH
DEVELOPMENT FOR THE LARGE AREA SILICON SHEET TASK
OF THE LOW COST SILICON SOLAR ARRAY PROJECT

by

C. D. Graham, Jr., D. P. Pope, S. Kulkarni, and M. Wolf

University of Pennsylvania
Philadelphia, PA   19104

Final Report

covering the period May 12, 1976-August 11, 1977

April 14, 1978

ABSTRACT

Results of an experimental program investigating the hot workability of polycrystalline silicon are reported. Uniaxial stress-strain curves are given for strain rates in the range of 10^{-5} to 10^{1} sec^{-1} and temperatures from 1100 to $1380^{\circ}C$. At the highest strain rates at $1380^{\circ}C$ axial strains in excess of 20% were easily obtainable without cracking; although special preparation of the compression platens allows strains in excess of 50%. After deformations of 36%, recrystallization is completed within 0.1 hr. at $1380^{\circ}C$. When the recrystallization is "complete", there is still a small volume fraction of unrecrystallized material which appears very stable and may degrade the electronic properties of the bulk material. Texture measurements showed that the as-produced vapor deposited polycrystalline rods have a <110> fiber texture with the <110> direction parallel to the growth direction and no preferred orientation about this axis. Upon axial compression perpendicular to the growth direction the former <110> fiber axis changes to <111> and the compression axis becomes <110>. Recrystallization changes the texture to <110> along the former fiber axis and <100> along the compression axis.

Table of Contents

I. Introduction

This report describes the results of a program in which the mechanical properties of polycrystalline silicon were investigated with the goal of determining the feasibility of producing thin sheets for photovoltaic use by standard hot working operations, e.g. hot rolling.

At the start of this program very little was known about the mechanical properties of polycrystalline silicon. Indeed, a great deal is known about the plasticity of single crystalline silicon[1] since silicon is commonly used as a model material for studying the micromechanisms of plastic deformation. But no basic information such as a stress-strain curve or a creep curve was available from the literature on polycrystalline material.

Given the dearth of mechanical property information on polycrystalline silicon, it was necessary to formulate a series of questions, the answers to which would give increasingly more useful information about the hot workability of the material. The obvious first questions are:

1. How much can the material be deformed without cracking?

2. What stresses are required?

3. What temperatures are required?

Since the production of a thin sheet requires large thickness reductions, intermediate recrystallization anneals are necessary. This might occur during the hot working process itself, as for example in the hot working of steels, or it might require seperate treatments. This gives rise to additional questions:

4. Does polycrystalline silicon recrystallize?

5. What strains are necessary to produce recrystallization?

6. What temperatures and times are needed.

There are additional questions related to the nature of the polycrystalline material itself. Because of its volume increase upon solidification, a crack-free polycrystalline sample is difficult to produce by simply solidifying a molten mass. In fact, the only available high purity polycrystalline material is produced by chemical vapor deposition, a process which produces a highly anisotropic material, that is, the axes of the individual crystallites are not randomly oriented in space, but have a definite preferred orientation. This anisotropy is called a texture. So several additional questions are raised:

7. What is the texture of the starting material?

8. What is the texture of the deformed material?

9. What is the texture of the recrystallized material?

And finally one needs to know the answer to:

10. How do deformation and recrystallization affect the electronic properties of the material?

At the start of this program there was a small amount of information in the literature related to questions 1, 2 and 3, but nothing was known about 4 through 10.

In hot metal-working operations the strain rate is typically in the range of 10^{-1} sec^{-1} to 10^2 sec^{-1}, so if these operations are to be used as a model the deformation behavior of polycrystalline silicon should be investigated up to quite high strain rates. (Typical strain rates in tensile tests are around 10^{-3} sec^{-1}.) Only one previous worker, C.L. Kolbe[2,3], has investigated the mechanical behavior of polycrystalline silicon. He did this by encasing the silicon in a

molybdenum jacket and then subjecting the composite to standard hot rolling and extrusion operations at 1250-1350°C. The Mo jacket was subsequently removed by oxidation. He found that silicon could be rolled as thin as 0.02 inches; although substantial problems with cracking were encountered. It was not known if the jacket is necessary simply to prevent oxidation of the silicon or if it actually produces an additional hydrostatic stress in the silicon which retards cracking. Also it cannot be decided, based on Kolbe's work, whether recrystallization occurred at all. Nonetheless, Kolbe's work showed that poly-crystalline silicon can be subjected to large plastic strains and provided the encouragement we needed to proceed.

There is one piece of evidence in the literature on the recrystallization of Ge, another diamond cubic material, in a paper by M.S. Abrahams.[4] He showed that a single crystalline sample subjected to a number of rolling passes in a specially designed mill at 700-800°C becomes polycrystalline after a reduction of about 60%. This clear evidence for recrystallization indicated that silicon probably would also recrystallize at similar strain and homologous temperature levels.

The body of this report describes the work done at the University of Pennsylvania attempting to answer the ten questions listed above. The results provide unambiguous answers to all but #10.

The body of this report is arranged in the following way: The texture of the polycrystalline material is discussed first in section II since a knowledge of it is necessary for all later discusion. The deformation experiments are then discussed in section III. A discussion of some experiments related to the susceptibility to edge cracking of silicon during rolling operations as determined by the forming

limit diagram follow in section IV. The recrystallization data are in section V and the diffusion length measurements are reported in section VI.

II.   Texture Measurements

The material used as samples in these texture measurements was
commercially available, high purity semiconductor grade silicon.
This is a polycrystalline material grown by chemical vapor deposition
at about 1150°C by hydrogen reduction of trichlorosilane[*]. The silicon
rod samples of about 15 cm diameter were prepared by the Dow-Corning
Company. Figure 1 shows the grain structure of a cross section of
the silicon rod. Growth begins on a core, the slim rod, from which
columnar grains elongated in the growth direction are clearly visible;
many of the grains show a substructure of straight, parallel needles
aligned with the growth direction. The appearance of these needles
suggests the possibility of growth twins, but they have not been
studied in detail. The over-all structure strongly suggests a pre-
ferred crystallographic texture in the as-deposited rod. Such a
texture is of obvious importance in measurements of the mechanical
properties, and since we were unable to find in the literature any
determination of the texture, we undertook the study described here.
And since deformation and recrystallization textures are commonly
observed in metals, a study of these textures was also made on poly-
crystalline silicon.

Samples for measurement of the as-received texture were cut
in various orientations and from various parts of the as-received
polycrystalline rod (see reference 5, included here as Appendix I,
for a complete description). The samples were cut with a diamond
saw, mechanically polished, and heavily etched in a solution of

---

[*]Verbal communication from Dr. James McCormick of the Dow-Corning Corp.

$5HNO_3: 3HF: 3CH_3COOH$. Measurements made on sample surfaces containing the polylog axis and the columnar grain axes will be described here.

Samples for deformation and recrystallization in the form of cylinders 12 mm long and 8 mm in diam were cut from the polycrystalline log using a diamond core drill. The axis of the sample cylinder was parallel to the axis of the log, and the cylinders were cut at positions well away from the center of the log. The radial grains of the log were thus approximately linear grains in the test cylinders, with the grain axes parallel to one another and perpendicular to the cylinder axis (see Fig. 2a).

The samples used in this work were compressed 30 pct axially at a strain rate of about 0.08 s^{-1} at $1380^{\circ}C$. A screw-driven Instron testing machine was used, with platens of Ta-10 pct W. (The rig is described more completely in section III and is illustrated in Fig. 7.) The sample cylinder was in an argon atmosphere, and was heated by an rf coil and a graphite susceptor. The total time required for the deformation was about 5 s, and the maximum applied stress was about 175 MPa. The samples were cooled to room temperature immediately after compression at an initial cooling rate of at least $200^{\circ}C/min$. The compressed samples were somewhat barrel-shaped because of friction forces at the platens, and in addition became elliptical in cross-section, as shown in Fig. 2b. The minor axis of the ellipse was the fiber axis of the original material. No cracking of the sample surfaces was observed in any of the tests. Each sample was annealed for 20 min at $1380^{\circ}C$ prior to compression, to attain a stable structure and grain size.

Annealing to bring about recrystallization was carried out in the same apparatus used for hot compression. In some cases the samples were annealed immediately following compression, and

in other cases sections cut from the compressed cylinders were
used for texture determination, as described below, and the
sections were then annealed.

Crystallographic textures were determined using the Schultz
back-reflection method[7] and a Siemens texture goniometer. Since
a sample with an area of at least 22 by 22 mm was required for
texture determination, four identical compression samples were
prepared for each determination, and from these samples there were
cut with a diamond saw a sufficient number of rectangular plates,
each 0.7 mm thick, to make up the necessary area. These plates
were cut with their major surface perpendicular to the compression
axis, except as noted below, and were taken from the central portion
of the sample cylinder to avoid complications resulting from friction
forces at the platens. These small plates, 12 to 20 in number, were
assembled into a composite specimen at least 22 by 22 mm in size,
mechanically polished flat, and etched in the same reagent as used
above. This composite sample was used for texture determination.
In some cases, the individual plates were rearranged into a different
order, and the texture was redetermined. There was no significant
difference in the measured textures. In the case of the as-received
material, a whole sample could be cut from the log since there was
no shortage of material.

The diffracted intensities were normalized with respect to a
random polycrystalline silicon sample made from powder, and plotted
on a pole figure. The reference direction of the pole figures is
the <110> fiber axis of the original polycrystalline material (see
Fig.2), except as noted below. Uncertainties in reading the dif-

fracted intensities from the strip chart of the apparatus lead to uncertainties of ± 0.1 deg in the radial direction and ± 7 deg in the azimuth of the pole figures. Complete details on the deformation and recrystallization texture measurements are contained in reference 6 (Appendix II).

The starting texture of the polylog material is shown in figure 3 in the form of a (220) pole figure with the 90-270° line along the length of the needle-like grains. This shows that the material has a sharp <110> fiber texture, with the <110> direction parallel to the growth direction (along the grain axes) with no preferred orientation about this axis. This same <110> texture has been found in silicon films grown by similar methods on various substrates[8]. This texture was not changed by annealing for times up to several hours at 1380°C, although the grain size was substantially increased up to a maximum of approximately 3 mm.

The textures which result from deformation and recrystallization are summarized in figure 4. It is seen that the 30% deformation has totally changed the texture to one with a <111> axis along the columnar grains (formerly a <110> axis) and the compression axis is now a <110> axis. Recrystallization completely changes the texture again, now with a <110> axis again along the length of the original columnar grains and a <100> along the compression axis. Two additional experiments were performed to see if the deformation and recrystallization textures are dependent on the starting textures: A previously deformed and recrystallized sample was again deformed and its texture determined. The same deformation texture as before was observed. Another sample was compressed and annealed then compressed and annealed again. The recrystallization texture was

also the same as before but stronger. Thus the deformation and recrystallization textures appear to be independent of the starting state. A detailed discussion of this is given in reference 6, included in this report as Appendix II.

The (220) pole figure of the deformed material and the (200) pole figure of the recrystallized material are shown in figures 5 and 6. These pole figures along with figure 3 provide the bases for figure 4. Note that the reference axis is parallel to the original columnar grains in each case. The influence of strain rate on texture was not investigated; although for strain rates above 8×10^{-3} at 1380°C there is little dynamic recovery and therefore the textures would not be expected to change.

The recrystallization texture shown in figure 4 is very likely the one which would be produced upon recrystallization of a rolled strip. Thus in a rolled and recrystallized sheet there would be a strong tendency for (100) planes to lie in the plane of the sheet, making it possible to increase the absorption of incident light in a photovoltaic cell by etching to produce needles, with <100> axes and (111) facets on the sheet surface.

III. Deformation Experiments

The purpose of these experiments was to investigate the extent to which polycrystalline silicon can be deformed without cracking and to measure the stresses necessary to produce various strain rates as a function of temperature. Strain rates typically used in rolling operations are in the range of 10^{-1} to 10^2 s^{-1}, so one goal of this work was to deform samples in this strain rate range. Uniaxial compression was chosen as the deformation mode since it is the most easily produced deformation state. Plane strain compression is more typical of the strain state produced by a rolling operation, but since plane strain compression experiments are more difficult and time consuming, it was decided that the more simple uniaxial compression experiments should be performed.

The experiments were performed in two standard testing machines, an Instron Universal Testing Machine for strain rates of 3 x 10^{-2} s^{-1} and below, and a CGS servo-controlled hydraulic testing machine for the higher strain rate tests. The results obtained on the two machines were identical when the strain rates were the same, except that when the Instron machine was used for strain rates above 3 x 10^{-2} s^{-1} recording system difficulties were encountered.

The apparatus used for temperature and environmental control is shown in figure 7. As shown in figure 7, the sample, #5, is compressed between Ta - 10%W platens, #4 & #6, which are in turn driven by stainless steel push rods, #1 & #7, with intervening layers of pyrolytic graphite, #3, for thermal insulation, and alumina, #2, for electrical insulation. The entire system is enclosed in a quartz tube, #8, with O-ring seals to the push rods, through which argon

gas circulates. The system is heated by rf coils, #10, driven by a 5KVA generator, which couple to a graphite susceptor, #9, within the chamber. The sample temperature is measured with a quartz-enclosed Pt-10Rh thermocouple which passes through holes in the wall of the quartz tube, #8, and the susceptor, #9, and touches the sample. Just as the test begins the thermocouple is withdrawn slightly so that it does not touch the sample during the test. Uncontrolled thermal gradients prevented temperature control better than $\pm 10^o$C although the thermocouple was capable of more accurate measurement. The sample temperature can increase by as much as 20^oC during the deformation experiment due to the work done by the machine. This temperature increase limited the maximum steady-state temperature at which the sample was equilibrated prior to testing to 1380^oC, which is about 30^oC below the melting point. The temperature prior to the test is reported in all subsequent data.

A deformation experiment is performed by adjusting the testing machine to move one of the push rods at a certain velocity and for a fixed distance. The motion of the rod is then measured from the strip charts on the Instron machine (cross head motion is linearly proportional to the strip chart motion) or from an oscilliscope trace on the CGS machine, which records the output of an LVDT attached to the bottom push rod, and is a measure of strain. The force is measured by a load cell below the bottom platen and is also continuously recorded. The sample length change is converted to true strain (the natural logarithm of the ratio of the initial to final height) and the load is converted to true stress (the load divided by the instantaneous cross-sectional area). The instantaneous cross-sectional area was calculated assuming uniform strain and no volume change due to plastic flow.

Test samples were diamond core drilled from the polylog in the same manner and to the same size as described in the previous section. They were also etched prior to testing in the same way. Two sample orientations were tested, as shown in figure 8. The least commonly used orientation has the <110> columnar grain axes parallel to the compression axis, 8a, and the most commonly used orientation has the grain axes perpendicular to the compression axis, 8b. The samples oriented as in 8a remained circular in cross section (since the sample structure is axisymetric about the compression axis) as shown in the photograph above 8a, while the other sample orientation, became distinctly elliptical in cross section, (as shown in the photograph above 8b). This is due to the fact that the strain along the diameter parallel to the columnar grains is very small. The ellipticity, measured by the ratio of the strains along the major and minor axes, decreased with decreasing strain rate and increasing temperature. This ratio ranged from approximately 1.8 at high strain rates and low temperatures to 1.1 at low strain rates and high temperatures. When cracking did occur on the sample surface it was always seen to initiate on the surface perpendicular to the major axis.

Load-elongation curves for as-received (not annealed) samples having the two orientations are shown in the two top curves on figure 9. Samples compressed along the columnar grains showed a distinct yield point as shown in the upper curve of figure 9 while those compressed perpendicular to the grain axes showed no yield point. Annealing the sample in the compression apparatus for 20 minutes at 1380°C prior to compression resulted in a large decrease in yield strength, as can be seen by comparing curves (b) and (c) of figure 9.

Detailed measurements were made only on annealed samples, compressed normal to the columnar grains.

The stress strain curves for annealed samples compressed perpendicular to the growth axis are shown in figures 10, 11, 12, and 13 for compression temperatures of 1100, 1200, 1300 and 1380°C respectively. Since the onset of edge cracking is delayed to higher strains at higher temperatures and lower strain rates, the stress-strain plots could be extended to larger strains for those samples. To facilitate comparison of the sample response at different temperatures and strain rates, the stress at a strain of 0.1 is plotted as a function of strain rate and temperature in figure 14. The strain of 0.1 was chosen since it corresponds to a reasonable reduction per pass in a rolling operation as determined, typically, by friction considerations that limit the ability of the rolls to draw the material through if the reduction becomes too great. Some general trends are immediately apparent: (1) The stress is not strongly strain-rate dependent at lower strain rates. (2) The strain rate dependence of the stress becomes increasingly strong at higher strain rates. (3) As the temperature is decreased from 1380°C the stress becomes increasingly strain rate dependent.

At the highest strain rate (~ 5 s^{-1}) at 1300°C and 1380°C the stress is 175 and 210 MPa (25 and 30 ksi), respectively, not a high stress for rolling operations. The temperatures are, of course, extremely high, requiring the development of entirely new roll materials for use at these temperatures.

Data on the 1200°C steady state creep stress of <111> oriented single crystals from the work of Myshlaev et al[9] are also shown on figure 14. The close similarity between the data is believed to be coincidental, since we are comparing data on single crystals and polycrystals, although the general trends of the data would be expected in the two cases.

IV. Forming Limit Diagram

In order for a material to be rollable, several conditions must
be met. First, the material must undergo substantial reduction in
thickness by rolling without cracking. Cracking normally occurs
first along the edges of the strip, since this is where the local
stresses are tensile rather than compressive. In order to evaluate
the rolling limit imposed by edge cracking, we have determined a pre-
liminary "forming limit diagram" for polycrystalline silicon. Such
diagrams have proven extremely useful in metal working applications[10],
and it is hypothethesized that they will also be applicable to silicon.

During the plastic deformation of a metal in a forming process,
the onset of fracture is determined by the maximum tensile strain and
the maximum compressive strain at the point of initiation of the frac-
ture. For the purposes of the analysis, the range of values of these
two strains are plotted on a "forming limit diagram" on which they
form a line. The diagram is then used in the following manner: If
the forming process is such that during deformation the strain co-
ordinates of all points in the material are such that the resultant
falls below the line, then the material will not fracture. If, how-
ever, the resultant at some point falls above the line, then the
part will fracture.

The diagram is determined by hot uniaxial compression of samples
as illustrated in figure 15. During high temperature compression,
the sample deforms from the shape shown on the left side of figure 15
to that shown on the right. As a result of this deformation w_o in-
creases to w and h_o decreases to h. The maximum tensile strain is

then given by $\ln (w_{max}/w_o)$ and the maximum compressive strain by $\ln (h_{max}/h_o)$. The values of these two strains are then plotted on the forming limit diagram. Different ratios of these strains are produced by using cylinders with different initial height to diameter ratios.

To measure the local strains in deformed silicon cylinders, grid lines like those of fig.15 were scribed on the samples with a diamond stylus. The sample was adhesively bonded to a cylindrical rod held in the chuck of a milling machine indexing head while the stylus was held in the milling machine chuck and spring loaded against the sample. The lines were then produced by rotating the sample under the stylus using the milling machine bed and indexing head motions. After scribing, the sample was lightly etched with the Sirtl etchant, to remove the grossly damaged material near the scratches which could nucleate cracks.

A preliminary forming limit diagram has been determined for annealed samples compressed parallel to the grain columnar axis at $1380^{\circ}C$ and $\dot{\varepsilon} = 8 \times 10^{-2}$ s^{-1}, shown in figure 15. It is a "preliminary" diagram since it consists of only three points, two of which are closely spaced. Since the diagrams determined on other materials have invariably had a slope of ½, the line for silicon was given that slope even through the data indicate a slightly higher slope. These three points were measured on samples which had length to diameter ratios of 0.81, 0.89 and 1.75.

The forming limit diagram for polycrystalline silicon shown in figure 16 is very nearly the same as that for 303 stainless steel at room temperature (see reference 10). This means that silicon at

1380°C with the texture used in these experiments would have about the same propensity for edge cracking as 303 stainless steel at room temperature. It should be emphasized, however, that this study is only preliminary and further work is needed.

Towards the end of this program a series of samples were deformed at strain rates between 1 and 10 sec^{-1} at temperatures above 1300°C to strains necessary to cause recrystallization. It was found that unless the Ta-W alloy platens and the sample faces were carefully polished prior to the test, the sample would "barrel" excessively and crack. The polishing allowed strains as high as 0.52 ($\dot{\varepsilon}$ = 7 sec^{-1}, T = 1340°C). This indicates that the forming limit diagram is strain rate dependent because samples can be deformed to these strain levels without special end preparation at lower strain rates, see figure 13. We have also shown that placing glass cover slides between the sample and platens greatly reduces the friction due to the viscous behavior of the soft glass at the test temperatures. For example, a sample of length to diameter ratio 1.5 compressed 30% at 1380°C at $\dot{\varepsilon}$ = 10^{-2} sec^{-1} without lubrication would normally develop edge cracks, but an identical sample, lubricated on the ends with a coverglass, and tested identically was deformed 40% with no sign of edge cracking. This lubricant also created problems since the glass extruded from between the sample and platen during the test and ran down the face of the sample. While these problems could, in principle, be controlled, we found polishing the platens to be simpler.

V. Recrystallization Studies

Poly-and Single-crystal bars of p-type silicon were provided by Dow Corning Corporation and Jet Propulsion Laboratories, respectively. The resistivity for the polycrystalline bars, which had been grown by vapour deposition, was quoted as 5 to 10 ohm-cm. In the case of the single crystals the resistivity was quoted as 10 ohm-cm. The polycrystalline material used in the experiments reported in previous sections of this report was undoped. See page 6 for sample dimensions.

Discs of a suitable thickness were cut perpendicular to the length axis of the logs and these were then ground to make the two flat surfaces parallel to each other to within 0.001 inches. The microstructure of one surface of each disc was examined after normal metallographic preparation followed by etching for 15 seconds in a solution of ratio 6:1:1 of nitric acid; acetic acid and hydrofluoric acid, respectively. Compression samples were core-drilled from these discs and etched in 5:3:3 solution made from 'electronic grade' nitric acid and hydrofluoric acid and 'reagent grade' acetic acid, respectively. After rinsing in deionized water, all the polycrystalline samples were annealed for 24 hours at $1380^{\circ}C$ in an evacuated quartz ampule. This procedure of etching in this 5:3:3 solution and rinsing in deionized water was carried out prior to any high temperature anneal or compression test.

Samples for metallographic examination were mounted in a cold-setting plastic and abraded on successively finer grades of SiC paper down to 600 grade. The samples were polished on 6μm diamond paste for about five minutes followed by further polishing for 1-2 hours

using 'Syton'[*] as the polishing medium. Good distinction between de-
formed and recrystallized regions was obtained by etching for about
5-10 seconds in 'Sirtl' etch. The 'Sirtl' etch was prepared fresh
each time by mixing 4 parts of solution A (50 g. of CrO_3 in 100 ml of
deionized water) with 3 parts of solution B (47-49% concentration
HF).

In order to systematically study the effect of each stage of
the process all the samples were cut and examined in one set manner.
Figure 16 illustrates the way in which samples were cut and the faces
that were examined by optical metallography.

The elongated grains radiating out from the center of the "poly-
log" bar indicate the growth direction of the crystals in the as-grown
material, as shown in figure 1; however in some areas the grains ex-
perience an abrupt change in their size and growth direction (figure
17). This is probably due to some change in the rate of deposition
of the vapour phase. Higher magnification micrographs of the silicon
samples in the as-received condition are shown in figure 18 for the
sections cut parallel and perpendicular to the compression axis.
Figure 18a shows a section similar to that in figure 1. But when
the sample is viewed along the growth direction of the polycrystals
(figure 18b) the 'Sirtl' etch reveals light regions on a dark back-
ground. The radial lines in the lightly-etched grains indicate the
nucleation point and the growth direction of the crystals. The dark
background is presumably comprised of a collection of much smaller
grains. Grain growth apparently does not occur during the deposition
process.

---

[*]Remet Chemical Corporation, P.O. Box 278, Chadwicks, N.Y. 13319

After annealing for 24 hours at 1380°C, the same cross-sections (figure 19) reveal that the darkly-etched regions have been removed to leave a fairly equiaxed structure. Some signs of the original elongated grains are visible when viewed in a section perpendicular to the compression direction (figure 19a) but most of these have been removed by the anneal.

Some samples were then annealed for 30 minutes at 1380°C in the compression rig to check for changes in the diffusion length as a result of contamination at this stage of the process. The platens were kept in contact with the silicon sample during heating with a preload of about 200 psi. Metallographic examination of these samples revealed a structure essentially identical to that of figure 19 both in regions near the center of the sample and near the surfaces in contact with the platens.

After the 24 hours pre-anneal the samples were compressed and re-examined. An interesting observation was made regarding the structure of two samples compressed by different amounts. Sample P50 was compressed to an average strain of $\varepsilon = 0.46$ ($\dot{\varepsilon} = 5.7$ sec^{-1}) and the series of micrographs on the as deformed material (figure 20) shows that some recrystallization had occurred whilst the sample was cooling in the compression rig. Sample P53 was compressed by an average strain of $\varepsilon = 0.36$ ($\dot{\varepsilon} = 4.5$ sec^{-1}) but a similar scan along the length of the specimen revealed only one area which had recrystallized in the rig. All other parts of the specimen exhibited the unclear, "cross-hatched", structure typical of the deformed grains. Since the specimens were treated in a similar way the difference between the two clearly suggests that the greater the total degree of deformation the more

readily the material will recrystallize.

To study the effect of annealing time at 1380°C after deformation, three times were selected, 0.1, 1.0 and 10 hours. Small pieces from specimens P50 and P53 were used for this purpose. Even after the short anneal of 0.1 hours at 1380°C, most of sample P53 appears to be recrystallized (figure 21); however, some debris from the deformation process appears to remain within some of the grains. This is clearly seen when these micrographs are compared with those from the samples annealed for 1 hour (figure 22) and 10 hours (figure 23). The observation of some darkly etched grains (even after annealing for 10 hours) and the grain size of sample P50 will be discussed later in this section.

Samples P54 and P56 were annealed for 10 hours at 1380°C, after compression, and sent to Jet Propulsion Laboratories for diffusion length measurements. These microstructures are shown in figure 24 and are essentially identical to those of specimen P53 (figure 23).

A graphic demonstration of the effect of degree of deformation on the ease of subsequent recrystallization is shown in figure 25 for a sample annealed for 1 hour at 1380°C. In a compression test the sample surfaces in contact with the platens experience a friction force which hinders the flow of metal during deformation. As a result, a gradient of the extent of strain is established along the length of the specimen; with the center having the most and the ends of the specimen having the least amount of deformation. It therefore follows that the greatest driving force for recrystallization will be at the center and hence this will recrystallize first. This is exactly as observed in figure 25, which shows that recrystallization

has occurred at the center of the sample but some deformed regions remain near the surface that was in contact with the platens. This is not considered to be a result of contamination from the platen material, since no such effect was observed in undeformed samples annealed in the rig. Unless otherwise stated, all micrographs presented in this report were taken near the center of the sample just so that these end effects could be discounted.

For samples pre-strained by $\varepsilon = 0.36$ (figure 21), recrystallization appears to occur within about 0.1 hours at 1380°C. However, some damage is still visible within several grains, suggesting that the process is not yet complete. Further annealing at this temperature removes most of the remaining strained regions.

Some grains, however, continue to exhibit the dark, heavily etched, contrast even after ten hours at 1380°C. It is suggested that these grains do not have sufficient deformation (i.e. driving force) for recrystallization to occur. This may be due to two possibilities. Firstly, these grains may be oriented along the 'hard' direction with respect to the stress-system within the polycrystal. If the surrounding grains are of a 'softer' orientation then they will deform and flow around the 'hard' grains, to comply with the externally imposed strain. The maximum load reached during the compression test will dictate the degree of deformation within these grains, but it will always be less than that in the softer orientated grains. On the other hand it is possible that these darkly-etched grains had a very high amount of deformation, and some recovery took place before the sample had time to cool, after the compression test. In this case, it is considered that the grains have relieved sufficient

internal damage such that a subsequent anneal will not affect them. The former suggestion is considered to be the more likely explanation since more darkly-etched grains are observed in sample P56, compressed by $\varepsilon = 0.36$, than in P54, compressed by $\varepsilon = 0.42$. Both samples had been annealed at $1380^{\circ}C$ for 10 hours.

The time of anneal in excess of the first 0.1 hours at $1380^{\circ}C$ does not appear to significantly affect the grain size of the silicon although the debris in the grain interiors tends to disappear with longer annealing times as can be seen by comparing figure 21 and 23.

VI. Diffusion Length Measurements

Samples were submitted to JPL for diffusion length measurements on two occasions. The first samples submitted were p-type material from a polycrystalline portion of a Czochralski boule supplied by JPL. These samples had a large grain size, more than 1 mm, which caused cracking during deformation. Consequently these samples could not be deformed enough to cause recrystallization during the subsequent annealing treatment. Not surprisingly these samples had diffusion lengths near zero. (The results of these measurements are described in a letter from Dr. Thomas Digges, Jr. to DPP dated May 19, 1977.)

A second series of experiments was then performed in the summer of 1977 in which p-type material, both polycrystalline and single crystalline, was given various treatments and then submitted to JPL for diffusion length measurements. (The material is the same as that described at the beginning of section V of this report.)

Single Crystalline Samples

Three pairs of samples were submitted to JPL for measurement. The first samples, P5 and P6, were simply cut from the JPL - supplied boule, etched and rinsed as described in section V, and sent to JPL. These two samples had diffusion lengths of approximately 30 microns. A second pair of samples, P1 and P2, was treated as described above, then annealed at 1380°C for 30 minutes under a preload of approximately 200 psi in the deformation rig. The diffusion lengths measured on these samples were zero within the range of experimental error. A third pair, P7 and P8 were treated as P5 and P6, then compressed

37% at 1353°C at a strain rate of 5 sec^{-1}, then annealed for 10 hours at 1380°C in evacuated quartz ampules. These samples also had near zero diffusion lengths. The results from samples P1 and P2 indicate that just holding the samples at elevated temperatures in the deformation rig results in diffusion length deterioration. Since the materials within the deformation rig are not of particularly high purity and furthermore some of these materials are heavy metals, e.g., Ta, W, Fe & Cr, such a deterioration is not totally unexpected. Unfortunately this deterioration prevented us from measuring the effects of deformation and recrystallization.

Polycrystalline Samples

Five batches of polycrystalline samples were submitted to JPL, all of which had very short diffusion lengths. Samples P46 and P47 were simply cut from the polylog, etched and rinsed as described above, and sent to JPL. The diffusion lengths were near zero. This is probably due to the very fine grain size in these samples (see figure 18). P40 and P41 were treated as above, then annealed in an evacuated ampule at 1380°C for 24 hours. These samples also had very short diffusion lengths, and one can only speculate on the reasons for this. Either the material became contaminated in the ampule or it still has too fine a grain size. Other samples which were just held in the deformation rig at 1380°C or deformed without recrystallization or deformed and recrystallized showed near zero diffusion lengths.

Since all the data pertinent to these diffusion length measurements are contained in Dr. Digges' letter of 9/26/77, it is produced in its entirety as Appendix III of this report.

It can be concluded from these measurements that simply holding samples in the deformation rig at 1380°C degrades their electronic properties. This is probably due to the presence of heavy metals and impure materials within the hot zone. The effects of annealing, deforming and recrystallizing the polycrystalline material are still unknown.

VII. Conclusions

The results of this program show that the plastic deformability of polycrystalline silicon is not very different from that of metals. The main differences lie in the stresses required (somewhat higher for silicon), the working temperatures required (higher for silicon), and the times needed for recrystallization (longer for silicon). Thus the properties of silicon differ from metals only in degree, not in kind.

Specifically we have shown that:

1. Polycrystalline silicon can be uniaxially compressed by as much as 50% at 1380°C without cracking. (Strains as high as 0.52 were obtained without side cracking at 1340°C, $\dot{\varepsilon}$ = 7 sec^{-1}.

2. At 1380°C a uniaxial stress of 1.7×10^8 Pa (25,000 psi) results in a strain rate of 5 sec^{-1}, well within the useful range for rolling operations.

3. Temperatures in excess of 1200°C are required for reasonable plasticity.

4. Polycrystalline silicon does recrystallize, and the texture produced upon recrystallizing a deformed sample has great potential use for photovoltaics.

5. Uniaxial strains of 30% are required to induce recrystallization.

6. At 1380°C recrystallization is nearly complete in 6 minutes. This indicates that separate recrystallization anneals are necessary since the recrystallization kinetics are not rapid enough to allow simultaneous deformation and recrystallization. Some small areas of apparently unrecrystallized material persist after as long as 24 hours at 1380°C, however.

7. The effects of plastic deformation and annealing on the electronic properties of the material have not been determined. It is possible that impurities introduced into the silicon from the deformation rig greatly degraded the properties, preventing such measurements.

8. It appears that silicon is capable of being rolled into thin sheets at temperatures above 1200°C.

9. The development of a rolling mill capable of performing this rolling operation constitutes a major program.

References

1. H. Alexander and P. Haasen, Solid State Physics, 22, 27 (1968).

2. J.F. Elliott, V.F. Meikleham and C.L. Kolbe, Energy Conversion for Space Power, Nathan W. Snyder, editor, Progress in Astronautics and Rocketry, 3, 263 (1961).

3. C.L. Kolbe, General Electric Research Laboratory Report No.63-RL-3221M (1963).

4. M.S. Abrahams, Trans. AIME, 230, 888 (1964).

5. B. Pratt, S. Kulkarni, D.P. Pope and C.D. Graham, Jr., J. Electrochem. Soc., 123, 1760 (1976).

6. B. Pratt, S. Kulkarni, D.P. Pope, C.D. Graham, Jr. and G. Noel, Met. Trans, 8A, 1799 (1977).

7. B.D. Cullity, Elements of X-Ray Diffraction, p.290, Addison-Wesley, Reading, Mass., 1956.

8. P. Rai-Choudhury and P.L. Hower, J. Electrochem. Soc., 120, 1761 (1973).

9. M.M. Myshlyaev, V.I. Nikitenko, and V.I. Nesterenko, Phys. Status Solidi, 36, 89 (1969).

10. P.W. Lee and H.A. Kuhn, Met. Trans., 4A, 969 (1973).

Growth Texture of Polycrystalline Silicon
Prepared by Chemical Vapor Deposition

Baruch Pratt,[1] Subhash Kulkarni, D. P. Pope, and C. D. Graham, Jr.

*Departments of Electrical Engineering and Science, and Metallurgy and Materials Science,
University of Pennsylvania, Philadelphia, Pennsylvania 19174*

We are undertaking a study of the high temperature deformation of polycrystalline silicon as part of a program to find low cost methods of manufacturing silicon solar cells. The material used as samples in these deformation experiments was commercially available,

high purity semiconductor grade silicon. This is a polycrystalline material grown by chemical vapor deposition at about 1150°C by the decomposition of trichlorosilane. The silicon rod samples were prepared by Dow-Corning Company, and had a diameter of about 15 cm. Figure 1 shows the grain structure of a cross section of the silicon rod. Growth begins on a single crystal core,

Fig. 1. Etched surface of 15 cm diameter silicon rod. Surface is perpendicular to log axis. Radial grains emanate from the slim rod.

the slim rod. Columnar grains elongated in the growth direction are clearly visible; many of the grains show a substructure of straight, parallel needles aligned with the growth direction. The appearance of these needles suggests the possibility of growth twins, but they have not been studied in detail. The over-all structure strongly suggests a preferred crystallographic texture in the as-deposited rod. Such a texture is of obvious importance in measurements of the mechanical properties, and since we were unable to find in the literature any determination of the texture, we undertook the study described here.

Experimental Procedure

A 2.5 cm thick slab was cut from the 15 cm diameter rod, perpendicular to the log axis. Samples for x-ray diffraction, each $2.5 \times 2.5 \times 0.2$ cm, were cut in various orientations and from various parts of the rod, as shown in Fig. 2. The samples were cut with a diamond saw, mechanically polished, and finally etched heavily in a solution of $5HNO_3 : 3HF : 3CH_3COOH$. Samples denoted $\perp$ were cut with their large faces perpendicular to the rod axis. Samples denoted $\parallel$ were cut with faces parallel to the log axis and perpendicular to a diameter. Those denoted $\parallel \parallel$ were cut with faces parallel to the log axis and parallel to a diameter. Sample sets 1
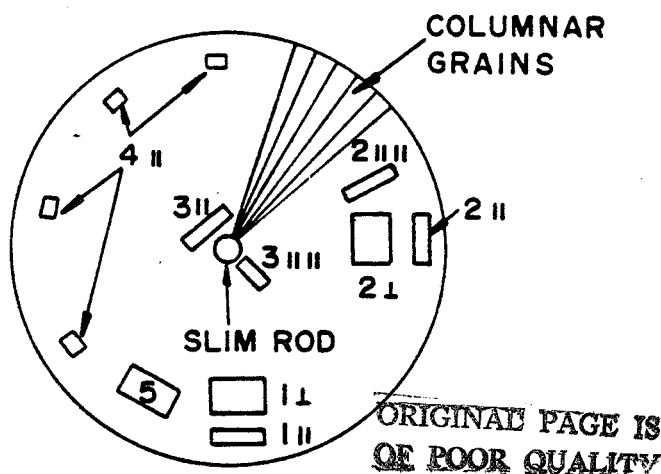
and 2 were taken near the log surface, at two points 90° apart. Sample set 3 was taken as near the slim-rod core as possible, and sample set 4 consisted of four pieces, each $0.6 \times 2.5 \times 0.2$ cm, and each cut with the 0.6×2.5 cm surface perpendicular to a log diameter. These four pieces were assembled to make one x-ray sample; this was done to minimize the spread in orientation resulting from the fanlike growth of the columnar crystals. Sample 5 was cut with faces inclined at 45° to the log axis; it has an orientation halfway between the $\perp$ and the $\parallel$ samples, related to them by rotation of 45° about an axis parallel to a log diameter. A small sample was also cut from the slim rod itself. Textures were determined by the Schultz reflection method (1, 2).

Samples were mounted in a Siemens texture diffractometer and irradiated with Cu K_α radiation at 30 kV and 20 mA. Reflections from (111), (220), and (400) planes were recorded, and pole figures were plotted from the resulting strip charts. Diffracted intensities were recorded for a full $\Psi = 360°$ rotation about the normal to the surface of the samples in steps of $\alpha = 2.5°$ away from this normal out to 80°. The resolution of the technique was $d\Psi = \pm4°$ and $d\alpha = \pm0.05°$. Intensities were compared to those of a random sample prepared from silicon powder held on a glass slide with petroleum jelly. The samples were aligned by eye so that the diameter of the log appeared as the vertical axis of the pole figures of the $\perp$ and $\parallel \parallel$ samples, and the log axis as the vertical axis of the pole figures in $\parallel$ samples.

Results

The recorder chart traces of all samples with faces parallel to a log diameter (types $\perp$ and $\parallel \parallel$) consisted of a series of very narrow peaks of high intensity. The small width of the peaks, plus the irregularities in their outlines caused by the relatively large grain size of the samples, made the plotting of conventional contour lines on the pole figures impossible. Instead, the height of each peak was read and plotted as a corresponding point on the pole figure. Examples are shown in Fig. 3.

All the pole figures from samples of type $\perp$ and $\parallel \parallel$ were in agreement, and indicated clearly that the crystallographic texture of the silicon rod is a very sharp $<110>$ fiber texture with the $<110>$ axis parallel to the growth direction, and with no preferential orientation about this axis. Pole figures of samples of type $\parallel$ unexpectedly showed almost random intensity instead of the circular symmetry about the midpoint expected for a fiber texture examined parallel to the fiber axis. Suspecting that this phenomenon might be associated with the spread in orientation of the fiber axis caused by the cylindrical growth geometry, we prepared the composite sample 4 as explained above; its (220) pole figure showed the expected form (Fig. 4) although with lower intensity than predicted.

As a final check, sample 5 was cut at 45° to the rod axis. The resulting (111) pole figure is shown in Fig. 5; it has the expected form of the (111) pole figure of Fig. 3a, rotated 45° about the equator.

The pole figures of sample set 3, cut near the central slim rod, were closely similar to those of sets 1 and 2. The slim rod itself was found to have a $<100>$ direction parallel to the rod axis.

Conclusions

The crystallographic texture of CVD polycrystalline silicon is found to be a very sharp $<110>$ fiber texture, with the $<110>$ direction parallel to the direction of growth, and with no preferred orientation about this axis. The texture does not appear to be influenced by the orientation of the rod from which growth starts. This $<110>$ growth texture has also been found in silicon films grown by similar methods on various substrates (3).

Acknowledgments

COLUMNAR GRAINS

SLIM ROD

Fig. 2. Identification of samples cut from silicon rod. For explanation, see text.

A1-3

1762   *J. Electrochem. Soc.:* SOLID-STATE SCIENCE AND TECHNOLOGY   *November 1976*
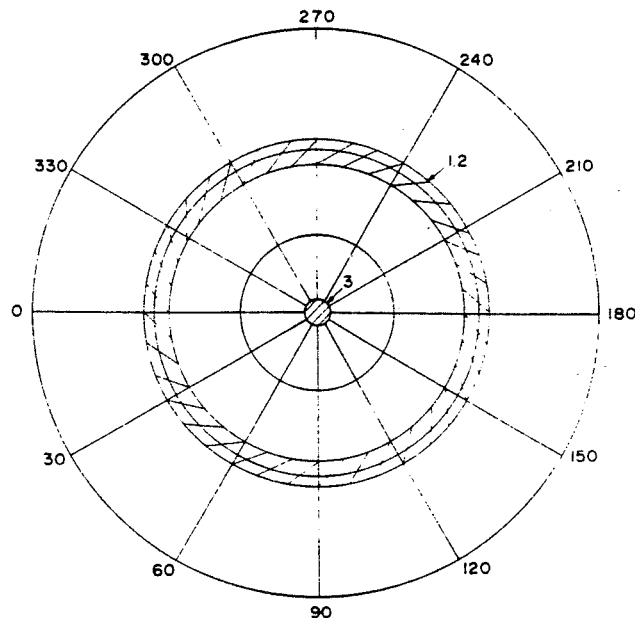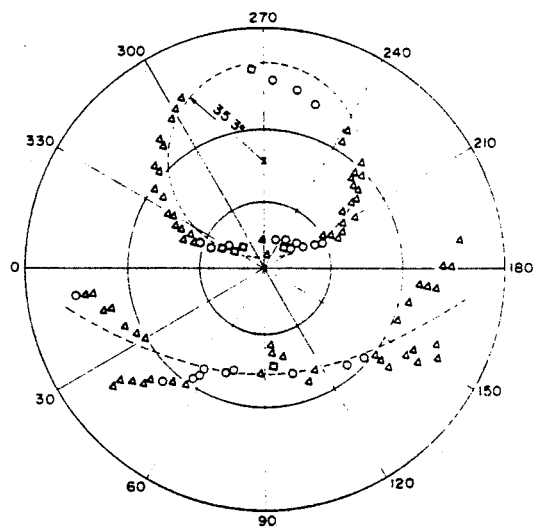
SYMBOLS
△ 1-2
○ 3-4
□ 5-6
▲ 7-8
● 9-10
■ >10

Fig. 4. Pole figure of composite sample 4 ||, for (220) reflection. Numbers indicate relative intensities as described in Fig. 3. Rod axis along 90°-270° line in the figure.

SYMBOLS
△ 1-2
○ 3-4
□ 5-6
▲ 7-8
● 9-10
■ >10

Fig. 5. Pole figure for (111) reflection of sample 5, cut at 45° to the rod axis. Intensities noted as in Fig. 3.

Any discussion of this paper will appear in a Discussion Section to be published in the June 1977 JOURNAL. All discussions for the June 1977 Discussion Section should be submitted by Feb. 1, 1977.

Fig. 3. Pole figures, (a, top) for (111), (b, middle) for (220), and (c, bottom) for (400) reflections plotted as multiples of the intensities observed on the random (powder) sample. For sample 2 || ||. Columnar grain axis along 90°-270° line in the figure.

They also thank the Department of Metallurgical Engineering of Drexel University for permission to use the

REFERENCES

1. L. G. Schultz, *J. Appl. Phys.*, **20**, 1030 (1949).
2. B. D. Cullity, "X-Ray Diffraction," p. 290, Addison-Wesley, Reading, Massachusetts (1956).
3. P. Rai-Choudhury and P. L. Hower, *This Journal*, **120**, 1761 (1973).

Deformation and Recrystallization Textures in Compressed Polycrystalline Silicon

B. PRATT, S. KULKARNI, D. P. POPE, C. D. GRAHAM, Jr., AND
G. NOEL

Cylindrical samples of polycrystalline semiconductor-grade silicon have been compressed 30 pct at 1380°C at a rate of 0.08 s⁻¹. The starting material had a strong ⟨110⟩ fiber texture, resulting from its growth by chemical vapor deposition; the fiber axis was perpendicular to the compression axis. The compression texture is very clearly defined after only 30 pct deformation, and has a ⟨110⟩ axis parallel to the compression axis and a ⟨111⟩ axis parallel to the original ⟨110⟩ fiber axis (perpendicular to the compression axis). Annealing for 10 min at 1380°C causes recrystallization. The recrystallization texture has a ⟨100⟩ axis parallel to the compression axis, and a ⟨110⟩ axis parallel to the original ⟨110⟩ fiber axis. Compression of a recrystallized sample gives the same deformation texture as does compression of the original material.

As part of a research program to determine the feasibility of hot-rolling silicon sheet for photovoltaic power generation, we have investigated the deformation of polycrystalline silicon by compression at temperatures from 1100°C to the melting point (1420°C), for a series of strain rates up to about 0.1 s⁻¹. In this paper we report on the crystallographic textures produced by compression and by recrystallization; the mechanical property data and metallographic results will be reported separately.

SAMPLE PREPARATION

The starting material was semiconductor grade polycrystalline silicon prepared by chemical vapor deposition (CVD) from trichlorosilane. The silicon was in the form of a "log" or cylinder about 150 mm in diam. The growth direction is radial, and the growth process results in columnar grain structure with the long axis of the grains everywhere parallel to the log radius. Previous work[1] has shown that there is a strong ⟨110⟩ fiber texture whose axis is parallel to the radial growth direction. This texture is not changed by annealing for times up to several hours at 1380°C, although the grain size is substantially increased (see Fig. 1).

Compression samples in the form of cylinders 12 mm long and 8 mm in diam were cut from the polycrystalline log using a diamond core drill. The axis of the sample cylinder was parallel to the axis of the log, and the cylinders were cut at positions well away from the center of the log. The radial grains of the log were thus approximately linear grains in the test cylinders, with the ⟨110⟩ grain axes parallel to one another and perpendicular to the cylinder axis (see Fig. 2).

The samples used in this work were compressed 30 pct axially at a strain rate of about 0.08 s⁻¹ at 1380°C. A screw-driven Instron testing machine was used, with platens of Ta-10 pct W. The sample cylinder was in an argon atmosphere, and was heated by an rf coil and a graphite susceptor. The total time required for the deformation was about 5 s, and the maximum applied stress was about 175 MPa. The samples were cooled to room temperature immediately after compression at an initial cooling rate of at least 200°C/min. The compressed samples were somewhat barrel-shaped because of friction forces at the platens, and in addition became elliptical in cross-section, as shown in Fig. 2. The minor axis of the ellipse was the ⟨110⟩ fiber axis of the original material. No cracking of the sample surfaces was observed in any of the tests.

Each sample was annealed for 20 min at 1380°C prior to compression, to attain a stable structure and grain size.

Annealing to bring about recrystallization was carried out in the same apparatus used for hot compression. In some cases the samples were annealed immediately following compression, and in other cases sections cut from the compressed cylinders were used for texture determination, as described below, and the sections were then annealed.

TEXTURE DETERMINATION

Crystallographic textures were determined using the Schultz back-reflection method[2] and a Siemens texture goniometer. Since a sample with an area of at least 22 by 22 mm was required for texture determination, four identical compression samples were prepared for each determination, and from these samples there were cut with a diamond saw a sufficient number of rectangular plates, each 0.7 mm thick, to make up the necessary area. These plates were cut with their major surface perpendicular to the compression axis, except as noted below, and were taken from the central portion of the sample cylinder to avoid complications resulting from friction forces at the platens. These small plates, 12 to 20 in number, were assembled into a composite specimen at least 22 by 22 mm in size, mechanically polished flat, and
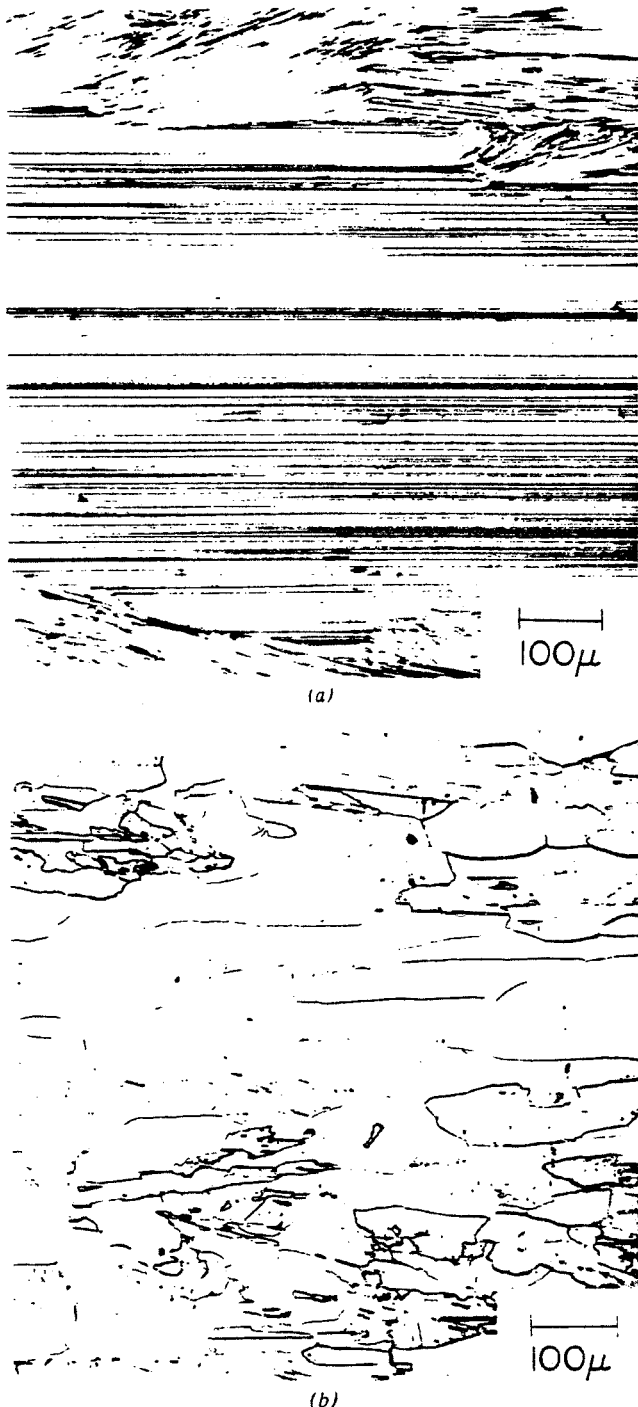
(a)

(b)

Fig. 1—Microstructure of CVD polycrystalline silicon. (a) As-deposited. Axis of elongated grains is a ⟨110⟩ fiber axis; (b) after annealing 20 min at 1380°C. Texture is unchanged.
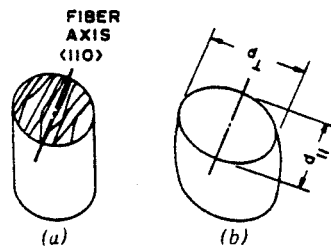

Fig. 2—Sample before and after compression, showing orientation of original fiber axis, and barreling and ellipticity after compression. The ratio of $d_\perp/d_\parallel$ is 1.15 after 30 pct compression at 1380°C.

etched in CP4 reagent. This composite sample was used for texture determination. In some cases, the individual plates were rearranged into a different order, and the texture was redetermined. There was no significant difference in the measured textures.

The diffracted intensities were normalized with respect to a random polycrystalline silicon sample made from powder, and plotted on a pole figure. The reference direction of the pole figures is the ⟨110⟩ fiber

(a)

(b)
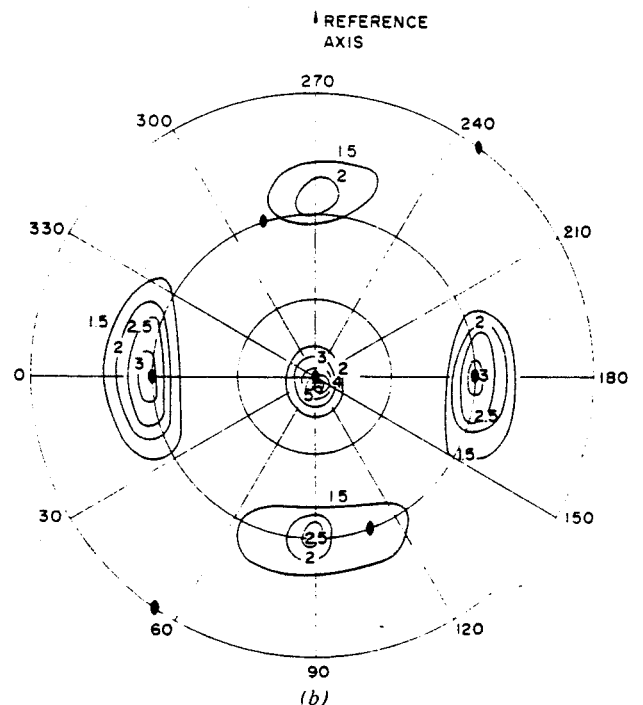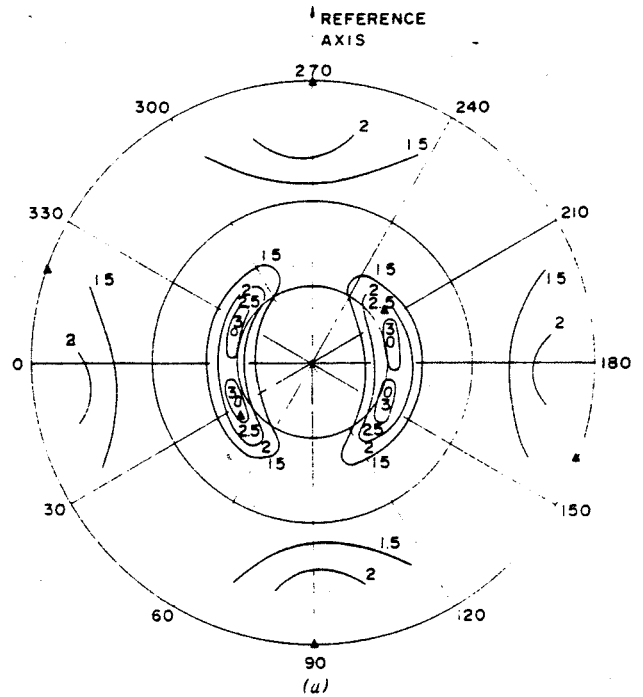
Fig. 3—(a), (111); (b), (220); and (c), (400) pole figures of CVD material compressed 30 pct at 1380°C at a rate of 0.08 s⁻¹. Section perpendicular to compression axis; reference arrow marks the original ⟨110⟩ fiber axis. Solid symbols are the ideal orientation described in the text.

ORIGINAL PAGE IS
OF POOR QUALITY

REFERENCE AXIS
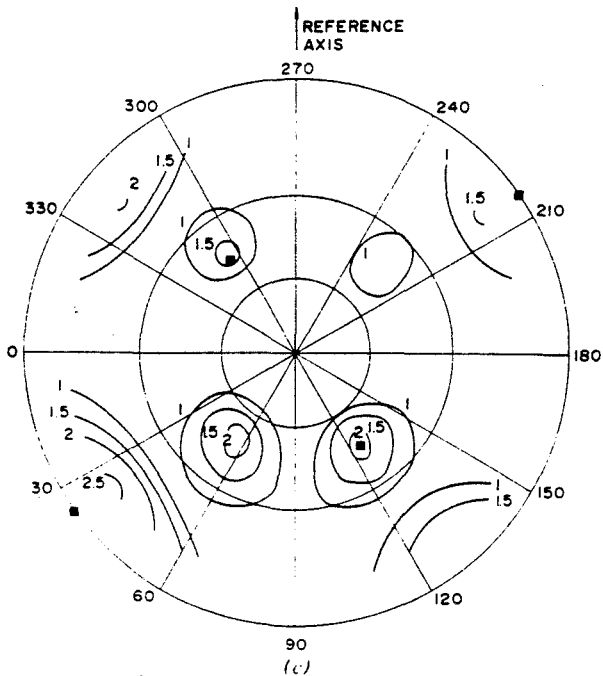
Fig. 3—Continued.

axis of the original polycrystalline material (see Fig. 2), except as noted below. Uncertainties in reading the diffracted intensities from the strip chart of the apparatus lead to uncertainties of ±0.1 deg in the radial direction and ±7 deg in the azimuth of the pole figures.

RESULTS

Figure 3 shows (111), (220), and (400) pole figures for the polycrystalline silicon deformed 30 pct in compression. Figure 4 shows (111) and (220) pole figures of samples deformed in the same way, but in this case diffraction is from a surface parallel to the compression axis and perpendicular to the original ⟨110⟩ fiber axis of the starting material. These figures establish that the deformation texture has a ⟨110⟩ axis parallel to the compression axis, and a ⟨111⟩ axis parallel to the original ⟨110⟩ fiber axis. This ideal orientation is indicated on each figure, and the agreement between the ideal orientation and the measured texture is generally good. In Fig. 4 the agreement is excellent. Traces of the original growth texture can be seen in the center of Fig. 4(b). The sharpness of the texture is surprising, in view of the relatively mild deformation of 30 pct. The ⟨110⟩ axis parallel to the compression axis is expected, since this is the normal compression texture for fcc metals,[3] and silicon is known to deform like an fcc metal despite its more complicated diamond cubic structure.[4] The metallographic and mechanical property evidence is convincing that recrystallization has not occurred during or subsequent to deformation, and that we are observing a deformation texture rather than a recrystallization texture.

Figure 5 shows (111), (220) and (400) pole figures of samples deformed just as for Figs. 3 and 4, but annealed for 10 min at 1380°C immediately following the deformation. A strong recrystallization texture has developed, which may be described as having ⟨100⟩

parallel to the compression axis and ⟨110⟩ parallel to the original ⟨110⟩ fiber axis (perpendicular to the compression axis). A trace of the deformation texture is seen at the center of Fig. 5(b). Continued annealing for several hours at 1380°C increased the grain size to several millimeters but did not alter the texture. Figure 6 summarizes the observed compression and recrystallization textures.

A sample compressed 30 pct and annealed to develop

(a)

(b)
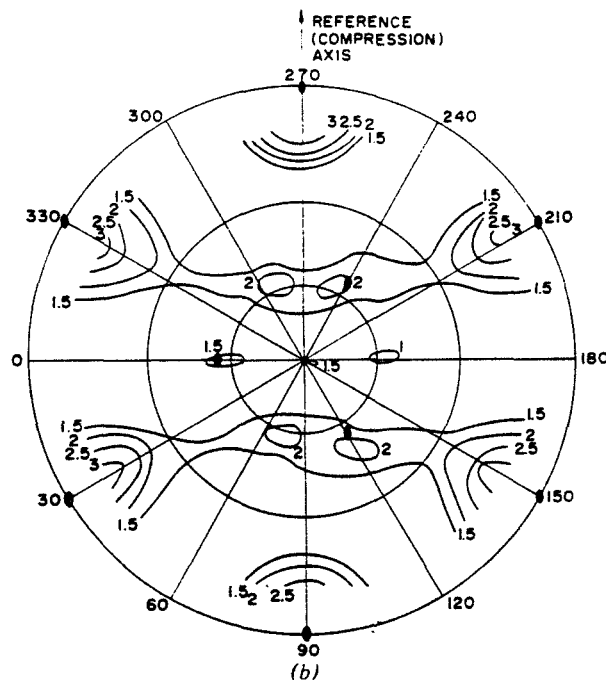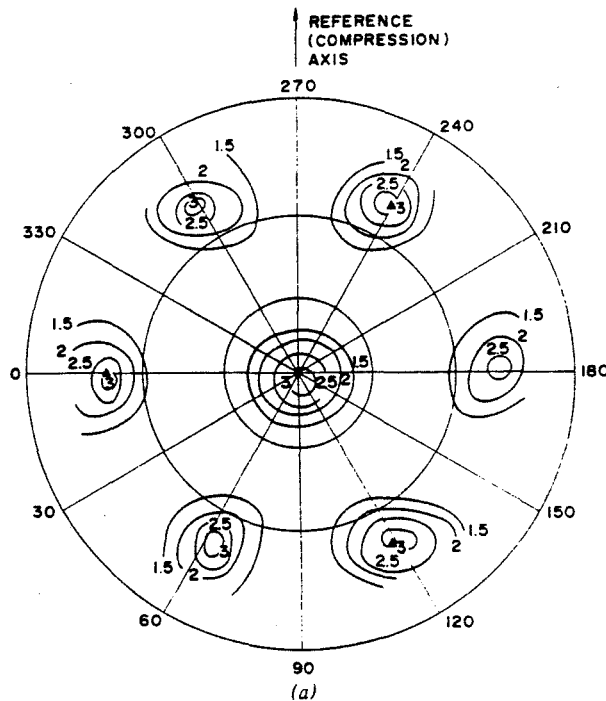
Fig. 4—(a), (111) and (b), (220) pole figures of sample compressed as for Fig. 3. Section parallel to compression axis. Reference arrow marks the compression axis: pole figure normal is parallel to original ⟨110⟩ fiber axis. Solid symbols are the ideal orientation described in the text. Note trace of starting texture at center of 4(b).

ORIGINAL PAGE IS
OF POOR QUALITY

the recrystallization texture was compressed an additional 30 pct at 1380°C. Figure 7 shows the (111) and (220) pole figures of this sample, viewed perpendicular to the compression axis, and Fig. 8 shows the (111) and (220) pole figures viewed parallel to the compression axis. Figures 7 and 8 show essentially the same texture as Figs. 3 and 4. The same texture thus develops after 30 pct compression from two very different initial textures. Again, traces of the starting texture can be seen at the center of Fig. 8(b).

(a)

(b)
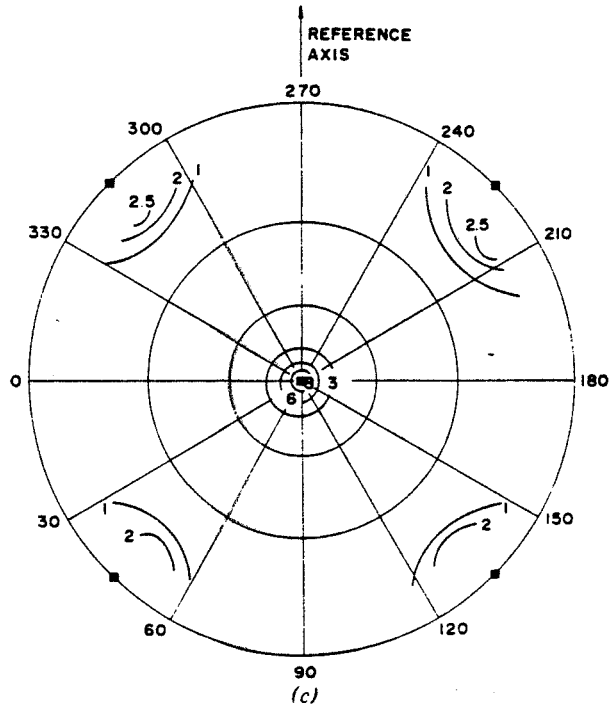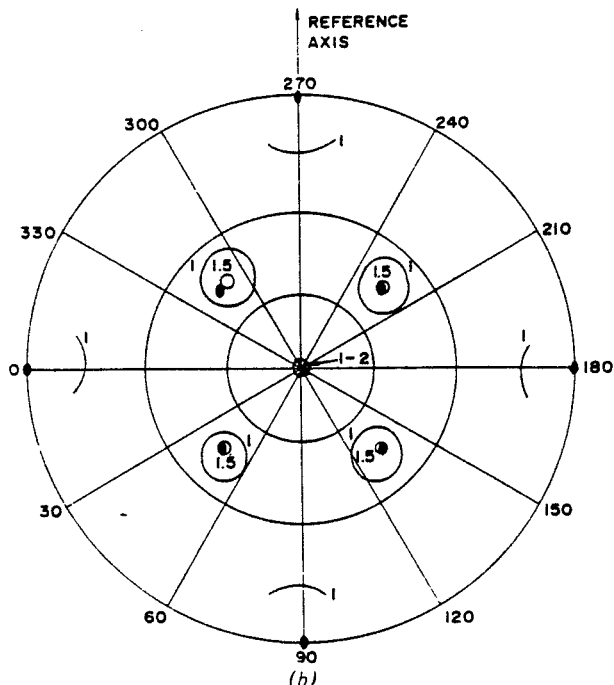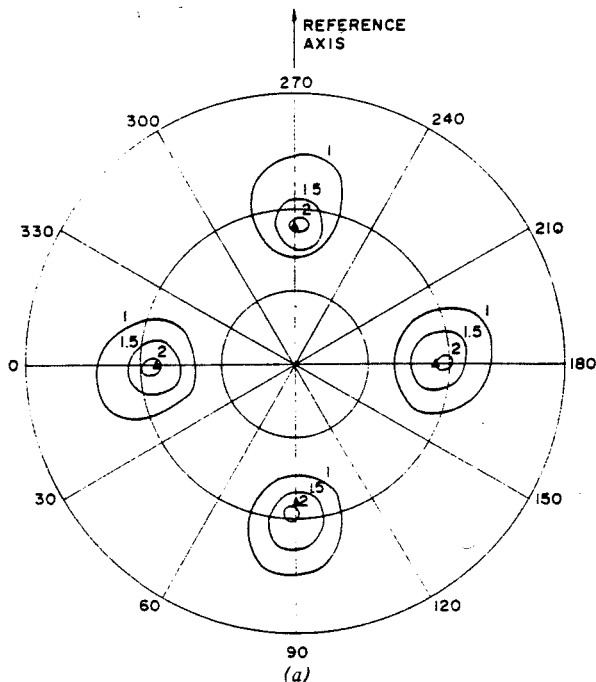
Fig. 5—(a), (111); (b), (220), and (c), (400) pole figures of samples deformed as for Figs. 3 and 4, then annealed 10 min at 1380°C. Section perpendicular to compression axis. Solid symbols are the ideal orientations described in the text. Trace of deformation texture visible at center of 5(b).

(c)

One cylindrical sample was alternately compressed and annealed at 1350°C to a final thickness of about 2 mm, corresponding to about 85 pct total compresssion. The final treatment was an anneal at 1300°C for 1 h. The texture of this sample was the same as that shown in Fig. 5, but with relative intensities about twice as high. Several hours of further annealing at 1350°C increased the grain size, but did not change the texture. Thus the recrystallization texture is not altered by repeated deformation and annealing cycles.

As a final check, one small plate from the texture sample of Fig. 4 and one from the texture sample of Fig. 7 were annealed for 10 min at 1380°C, and then a diffraction trace was taken with a conventional X-ray diffractometer (not a texture diffractometer). The plate from the sample of Fig. 4 showed a high value for the ratio of the (220) to the (111) peak, and the plate of Fig. 7 showed a high value for the ratio of the (400) to the (111) peak, as compared to the ratios in a random sample. This confirms the texture determination in both cases.

DISCUSSION

Since it seemed quite remarkable that such a strong deformation texture could be produced from such a strong initial texture, the following analysis was per-
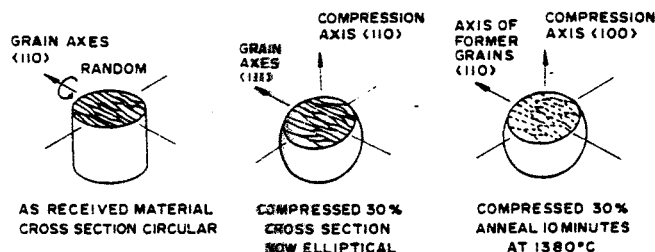
Fig. 6—Schematic illustration of starting texture, compression texture, and annealing texture.

formed. The starting sample consists of individual grains whose axes are $\langle 110 \rangle$ and are perpendicular to the compression axis (Fig. 6). This sample was then modelled as a collection of independent single crystals, each with a $\langle 110 \rangle$ reference direction (perpendicular to the compression axis), and with the compression axes located every 10 deg along the great circle forming the $\langle 110 \rangle$ zone. Each crystal was then assumed to deform in compression by 30 pct and the final orientation of each crystal was calculated using the method of G. I. Taylor.[5] It should be noted that some of the crystals deformed first by single slip until the compression axis reaches the $\langle 001 \rangle - \langle 011 \rangle$ symmetry line, after which they deform by polyslip. The results of this analysis are shown in the (111) pole figure of Fig. 9. This plot should be compared to Fig. 3(a). While the two figures are certainly not identical, certain similarities exist: the centers of the high intensity contours are in the same regions of the two pole figures and the symmetries are the same. But per-
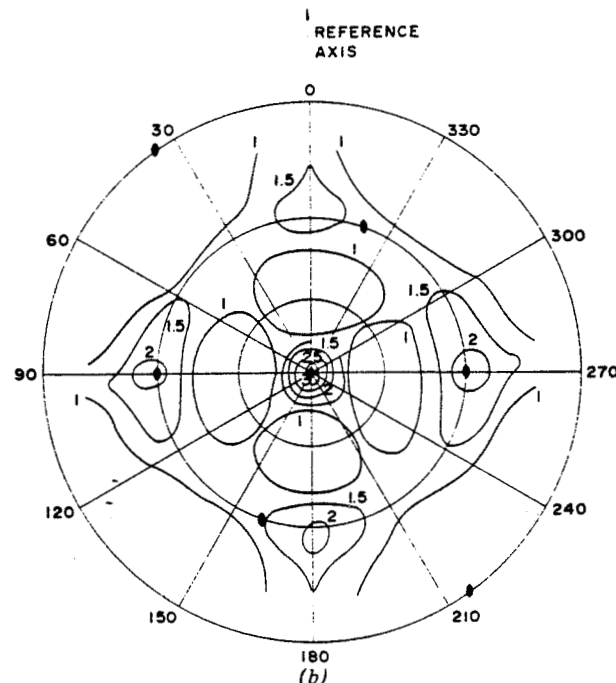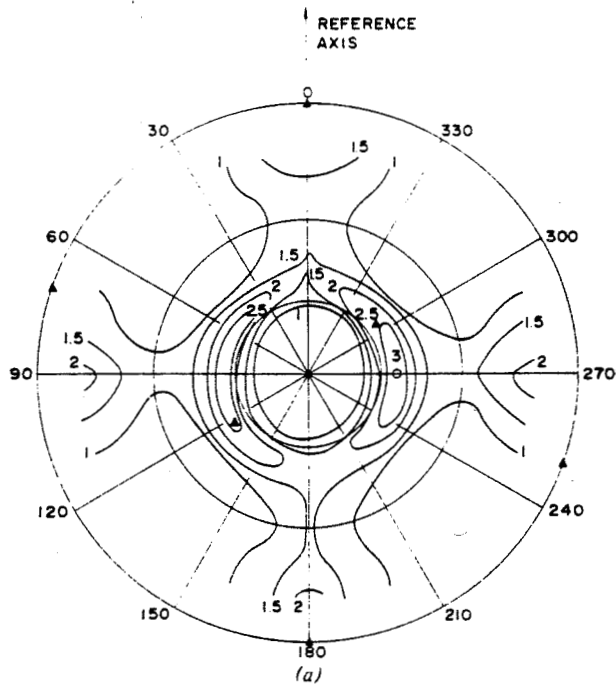
Fig. 7—(a), (111) and (b), (220) pole figures of sample treated as in Fig. 5, then compressed an additional 30 pct at 1380°C, 0.08 s⁻¹. Section perpendicular to compression axis; reference arrow marks original $\langle 110 \rangle$ fiber axis. Solid symbols are the ideal orientation described in the text.
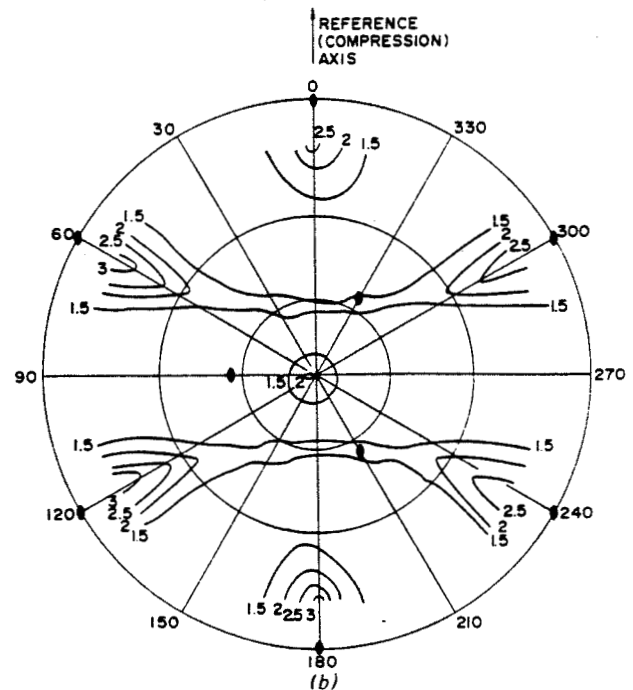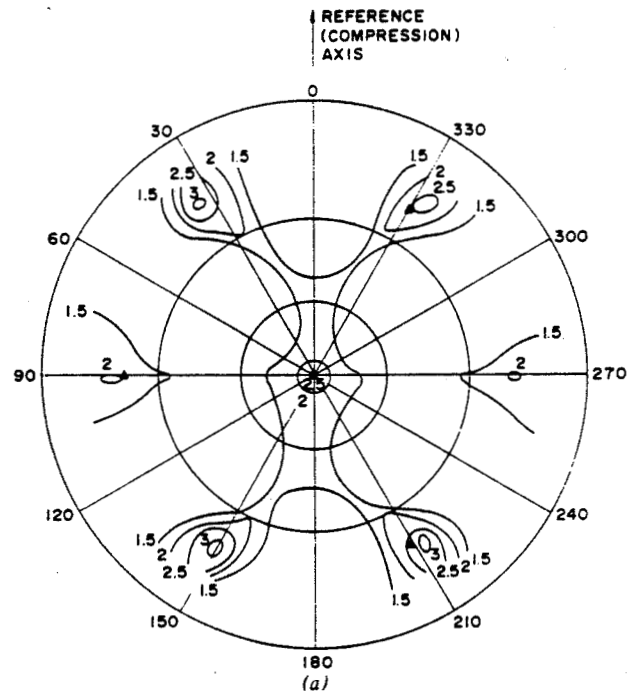
Fig. 8—(a), (111) and (b), (220) pole figures for section parallel to compression axis of sample treated as in Fig. 7. Reference arrow marks compression axis; normal to pole figure is the original $\langle 110 \rangle$ fiber axis. Solid symbols are the ideal orientations described in the text. Note traces of starting texture at center of 8(b).
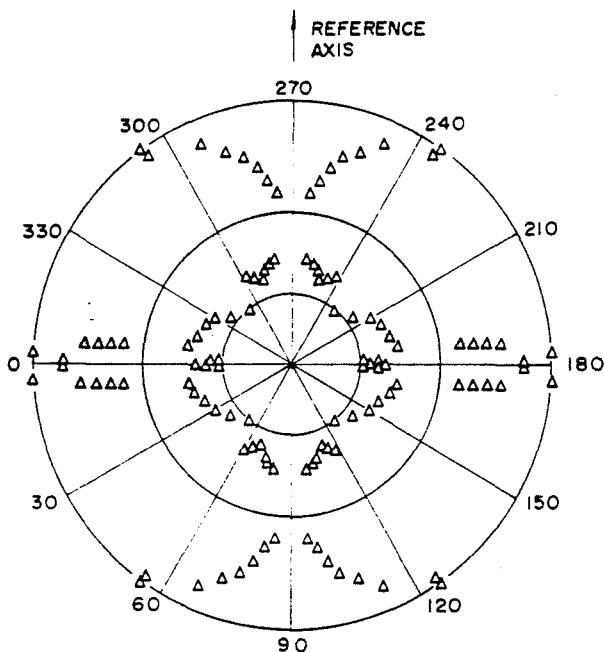
Fig. 9—Calculated (111) pole figure assuming that the sample consists of a collection of independently deforming crystals, each with an initial compression axis along the $\langle 110 \rangle$ zone. Reorientations were calculated for initial orientations every 10 deg between (001) and ($\bar{1}$10) along this zone. Compare to Fig. 3(*a*).

pression axis, and a recrystallization texture with $\langle 100 \rangle$ parallel to the compression axis and $\langle 110 \rangle$ parallel to the original $\langle 110 \rangle$ fiber axis, both give the same compression texture after 30 pct axial compression at 1380°C at a rate of 0.08 s^{-1}. The compression texture has a $\langle 110 \rangle$ parallel to the compression axis, and a $\langle 111 \rangle$ parallel to the original $\langle 110 \rangle$ fiber axis. Recrystallization, which is complete in 10 min at 1380°C, gives a texture with $\langle 100 \rangle$ parallel to the compression axis and $\langle 110 \rangle$ parallel to the original $\langle 110 \rangle$ fiber axis (perpendicular to the compression axis).

haps most important of all, the calculated pole figure in Fig. 9 shows a strong texture which is very different from the starting texture. Thus to a first approximation it appears that the deformation texture may be considered to arise from the expected rotations of the individual crystals, with the condition that the grains deform independently of one another. The relatively large grain size probably accounts for this behavior.

The elliptical cross-section of the compressed samples can be attributed to the fact that all of the predicted slip planes in the $\langle 110 \rangle$ fiber texture samples would contribute more strongly to an increase in the sample diameter perpendicular to $\langle 110 \rangle$ than parallel to $\langle 110 \rangle$.

SUMMARY

Two different starting textures in polycrystalline silicon, a $\langle 110 \rangle$ fiber texture perpendicular to the com-

ACKNOWLEDGMENTS

REFERENCES

1. B Pratt, S. Kulkarni, D. P. Pope and C. D. Graham, Jr.: *J. Electrochem. Soc.*, 1976, vol. 123, p. 1760–1762.
2. B. D. Cullity: *Elements of X-Ray Diffraction*, p. 290, Addison-Wesley, Reading, Mass., 1956.
3. C. S. Barrett and T. B. Massalski: *Structure of Metals*, 2nd ed., p. 547, McGraw-Hill, N. Y., 1966.
4. H. Alexander and P. Haasen: *Solid State Phys.*, 1970, vol. 22, p. 28ff.
5. G. I. Taylor: *Proc. Roy. Soc.*, A66, 1927, pp. 16–38.
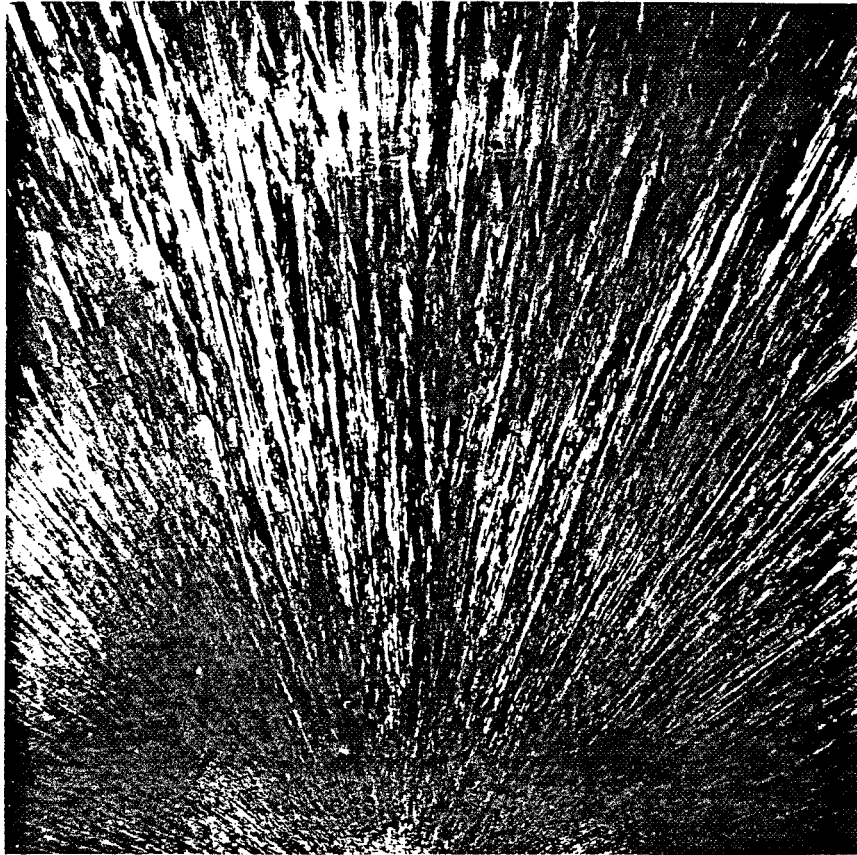
$\overline{5\,mm}$

Fig.1. Structure of vapor deposited poly-
crystalline silicon as seen in a
section perpendicular to the log
axis. The grain axes lie along the
growth direction and are <110>.

FIBER
AXIS
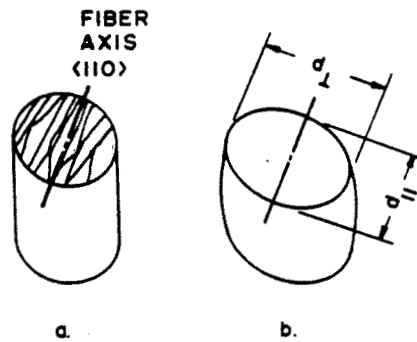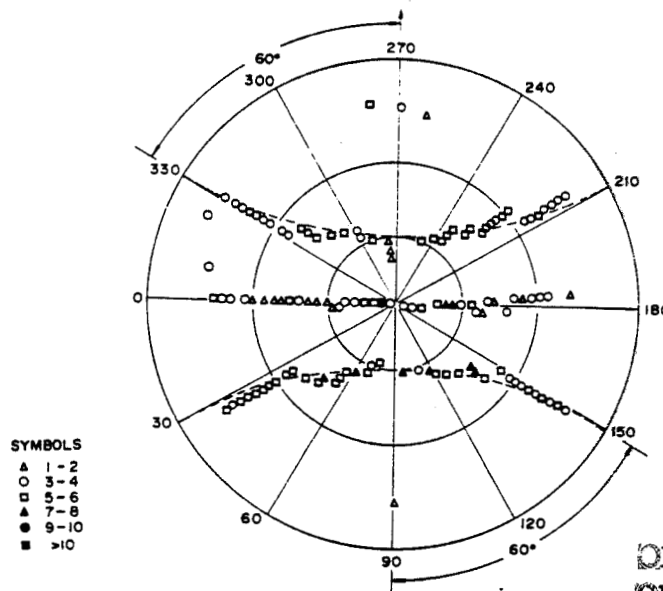⟨110⟩

$d_\perp$

$d_\parallel$

a.　　　　b.

Fig. 2. Sample before and after compression,
showing orientation of original grain
axis, and barreling and ellipticity
after compression. The ratio of $d_\perp/d_\parallel$
is 1.15 after 30% compression at 1380°C.
The grains shown in (a) are the same as
those seen in Fig. 1.

SYMBOLS
△ 1 - 2
○ 3 - 4
□ 5 - 6
▲ 7 - 8
● 9 - 10
■ >10

Fig. 3. Pole figure for (220) reflections
plotted as multiples of the intensi-
ties observed on a random powder
sample. Columnar axis along 90-
270° line. Sample face contains
grain axis and polylog axis. The
numbers associated with the symbols
indicate the ratio of the local
x-ray intensity to the random
background intensity.
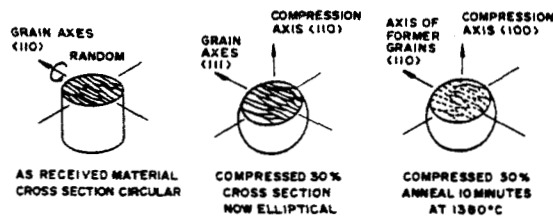
GRAIN AXES
⟨110⟩   RANDOM

COMPRESSION
AXIS ⟨110⟩
GRAIN
AXES
⟨111⟩

AXIS OF   COMPRESSION
FORMER   AXIS ⟨100⟩
GRAINS
⟨110⟩

AS RECEIVED MATERIAL   COMPRESSED 50%   COMPRESSED 50%
CROSS SECTION CIRCULAR   CROSS SECTION   ANNEAL 10 MINUTES
                         NOW ELLIPTICAL   AT 1380°C

Fig.4.   Schematic illustration of starting
          texture, compression texture, and
          annealing texture.
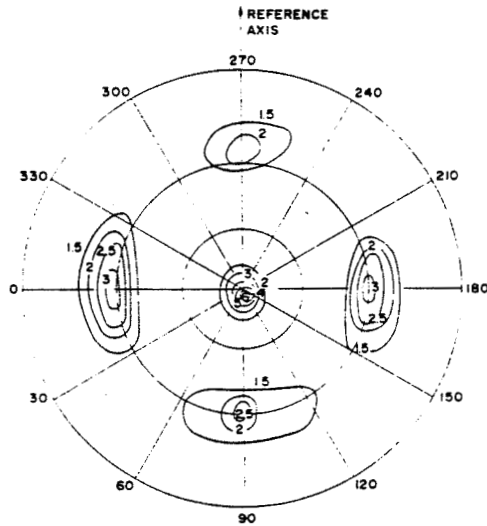
Fig.5.   (220) pole figure of CVD material
         compressed 30% at 1380°C at a rate
         of 0.08 sec⁻¹. Section perpendicular
         to compression axis; reference arrow
         marks the original <110> fiber axis.
         Solid symbols are the ideal orientation
         described in the text.
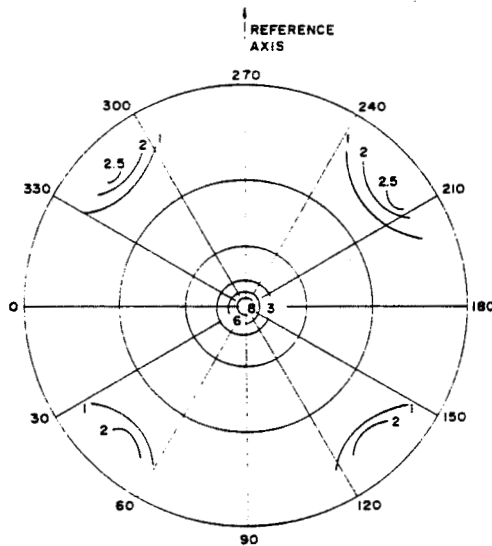
Fig.6.   (400) pole figure of sample deformed as
         for Fig.5, then annealed 10 minutes at
         1380°C. Section perpendicular to com-
         pression axis; reference arrow marks
         original <110> fiber axis.

(1) Top push rod to Crosshead
(2) Alumina disc
(3) Pyrolytic graphite disc
(4) Top platen (Ta + 10% W)
(5) Silicon sample
(6) Bottom platen (Ta + 10% W)
(7) Bottom push rod to load cell
(8) Quartz tube
(9) Graphite suscepter
(10) R. F. Heater coil
(11) Shielded thermocouple
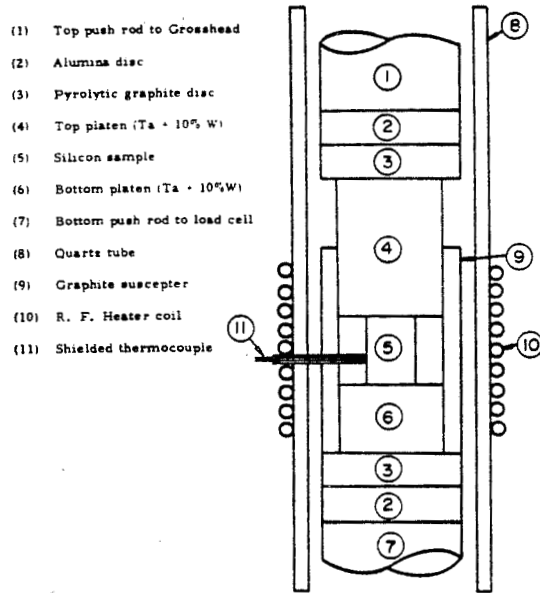
Fig.7. Schematic of the uniaxial compression
        rig.

grain axis ⟨110⟩
random

grain axis
⟨110⟩
random

(a)   (b)
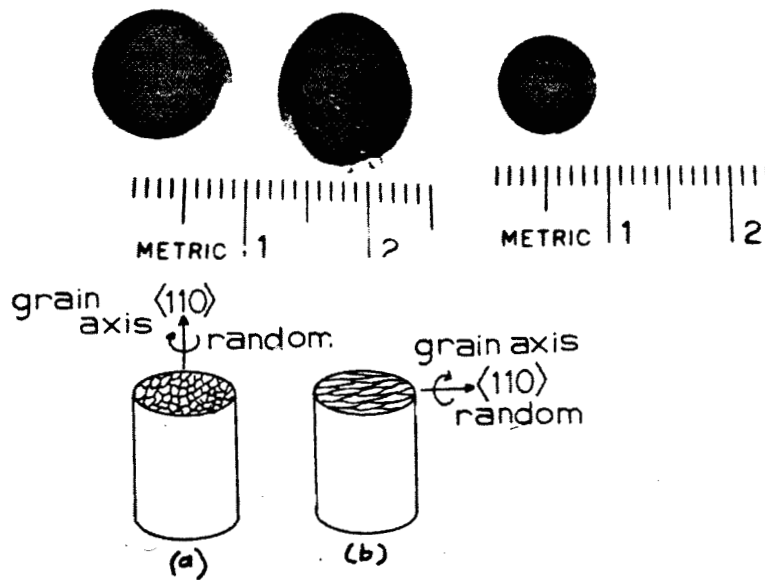
Fig. 8.   Sample orintations tested in uniaxial
           compression. Samples with columnar
           grains along the compression axis as
           in (a) remained circular in cross sec-
           tion while those oriented as in (b)
           became elliptical.
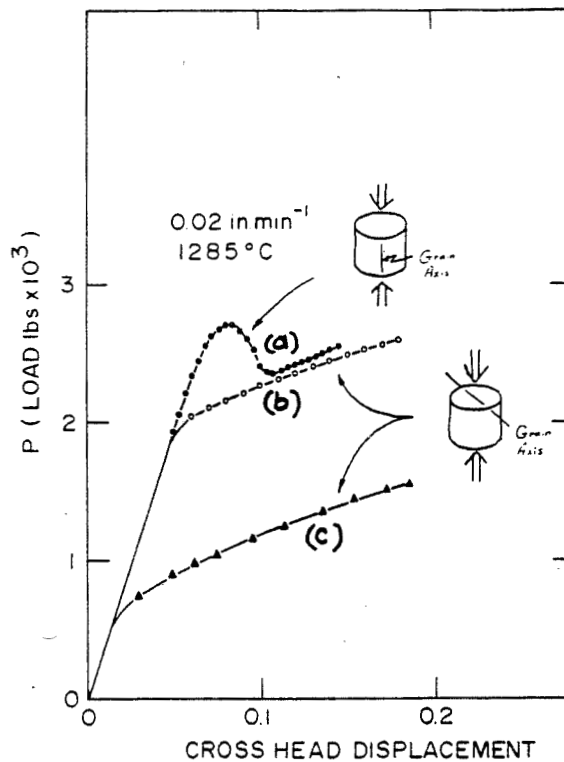
Fig.9. Load compression curves for two sample orientations. Curve (a) is for a virgin sample compressed parallel to the columnar grains, (b) is for a sample in the same condition but compressed perpendicular to the grains and (c) is for an annealed sample oriented as in (b). Note the large yield stress reduction upon annealing.
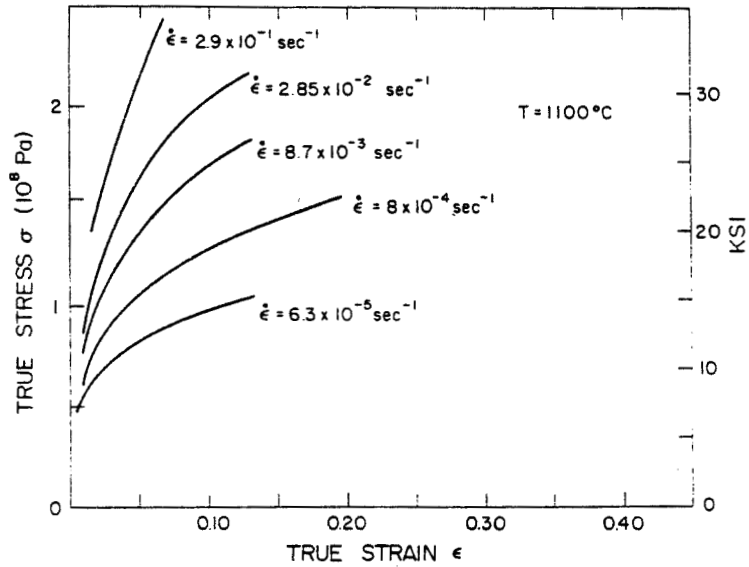
Fig.10.   True stress-true strain curves for samples deformed at 1100°C.
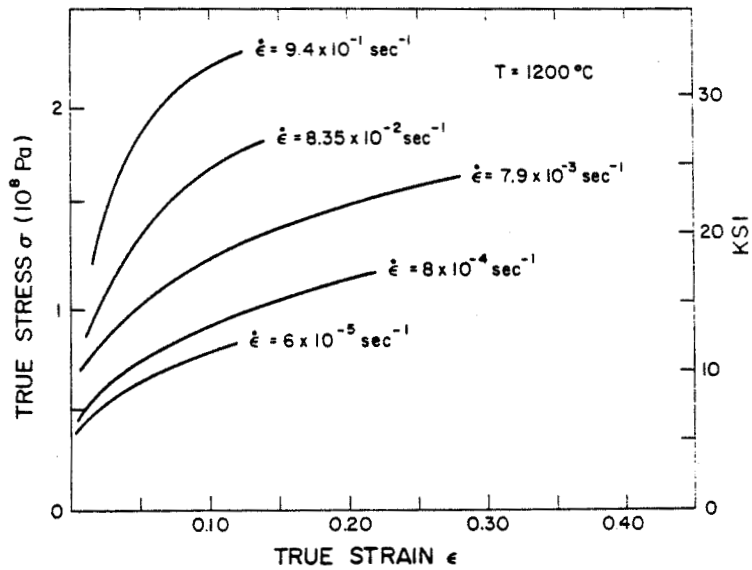
Fig.11.   True stress-true strain curves for samples deformed at 1200°C.
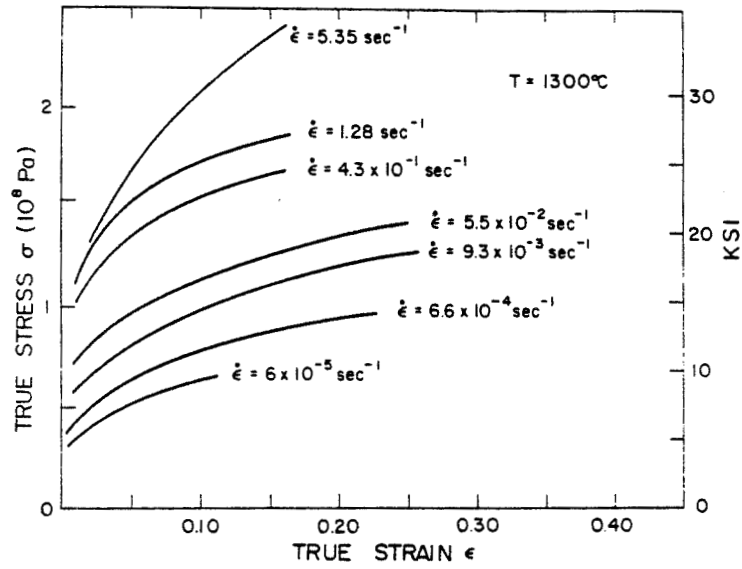
Fig.12. True stress-true strain curves for samples deformed at 1300°C.
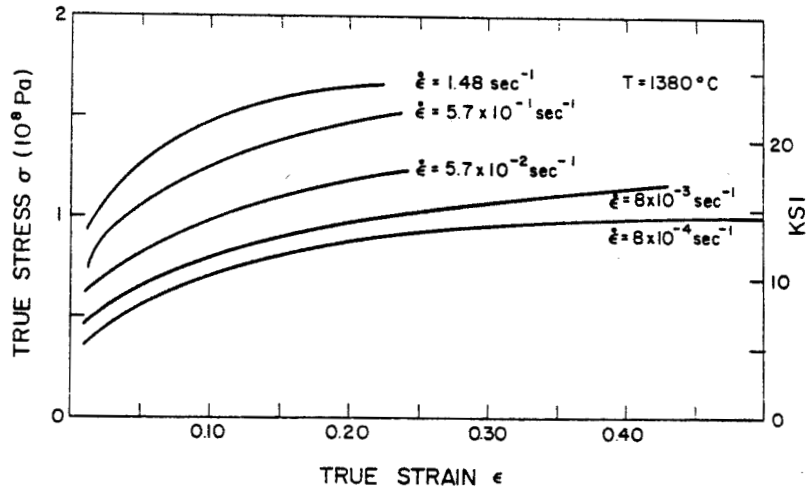
Fig.13. True stress-true strain curves for samples deformed at 1380°C.
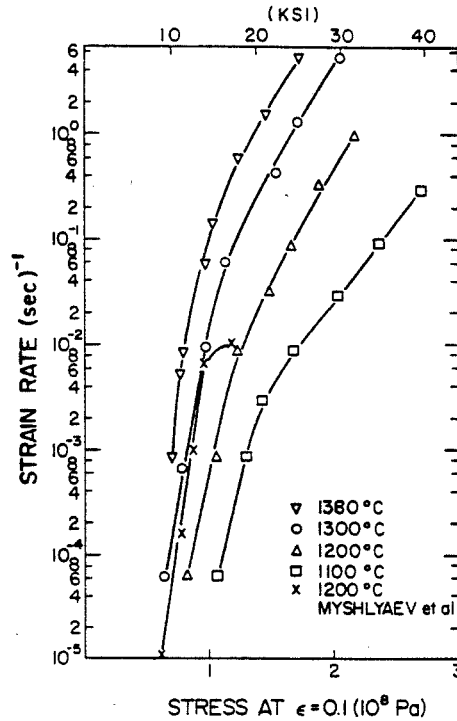
Fig.14. Stress vs strain rate (measured at a
strain of 0.1) for all temperatures
and strain rates. Note the correla-
tion with the Myshlyaev et al[9] data.
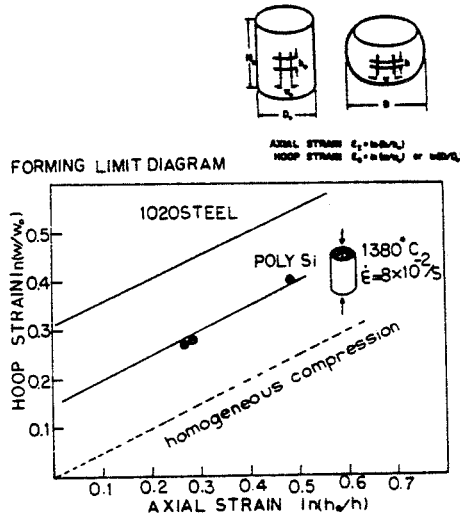
Fig.15. Forming limit diagram for polycrystalline sample
with grains orientated as shown. The line of slope 1/2
was drawn through the three points because forming limit
diagrams for metals have slope 1/2. The diagram shown for
mild steel is for room temperature. The schematic above
the graph shows how the strains are calculated from a
compression test.

(a)

(b)

Face
A (Platen
end)

Growth
Direction

Face
C

Face B

(c)

Face
B

Face
B

Face
C

Face A

Face C
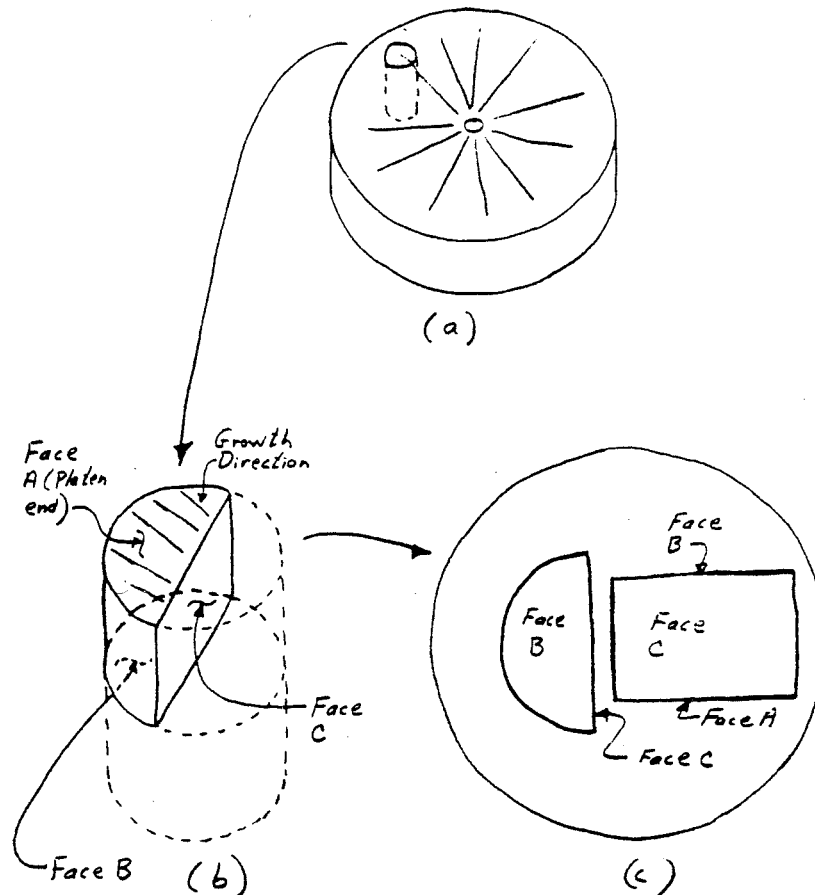
Fig.16.   A schematic showing how samples were
cut from the polylog (a), the section-
ing of the sample (b), and the placement
of the sectioned faces in the metallo-
graphic mount (c).
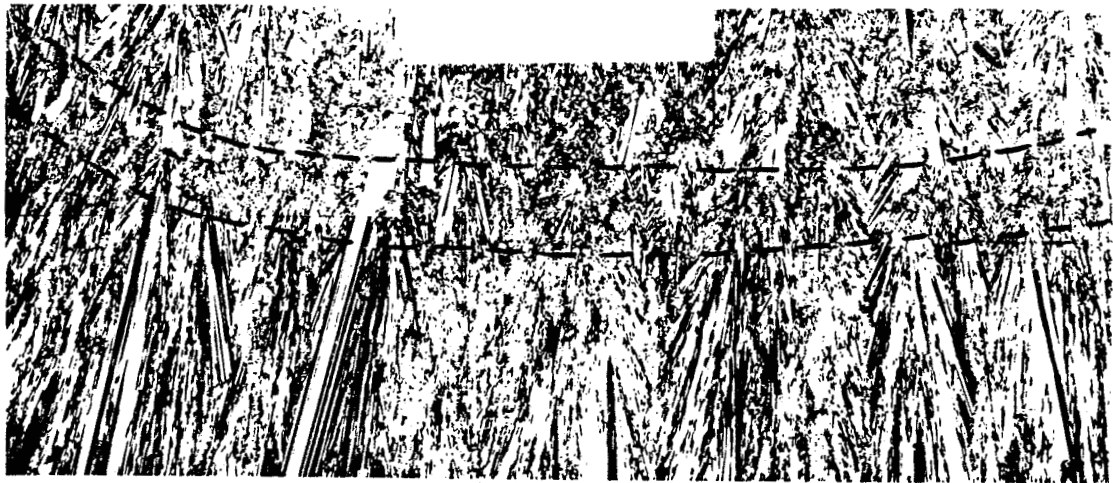
Fig. 17. A section through the polylog showing
an abrupt change in microstructure,
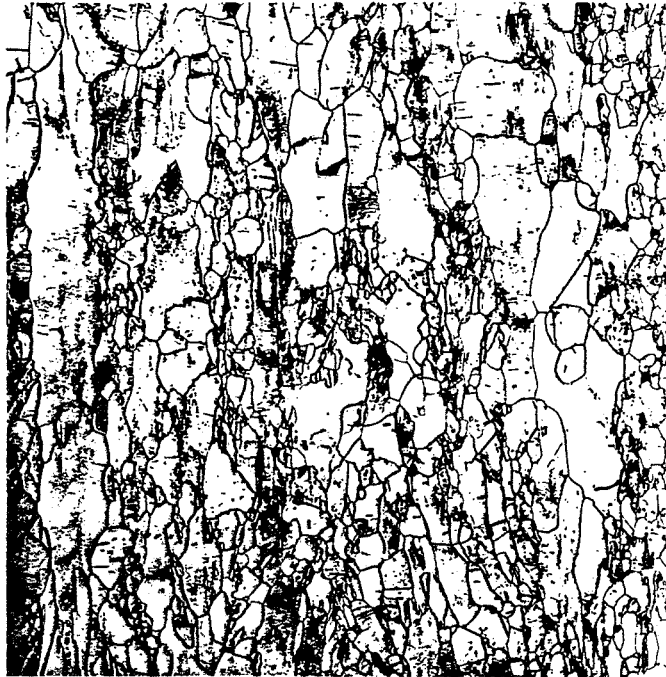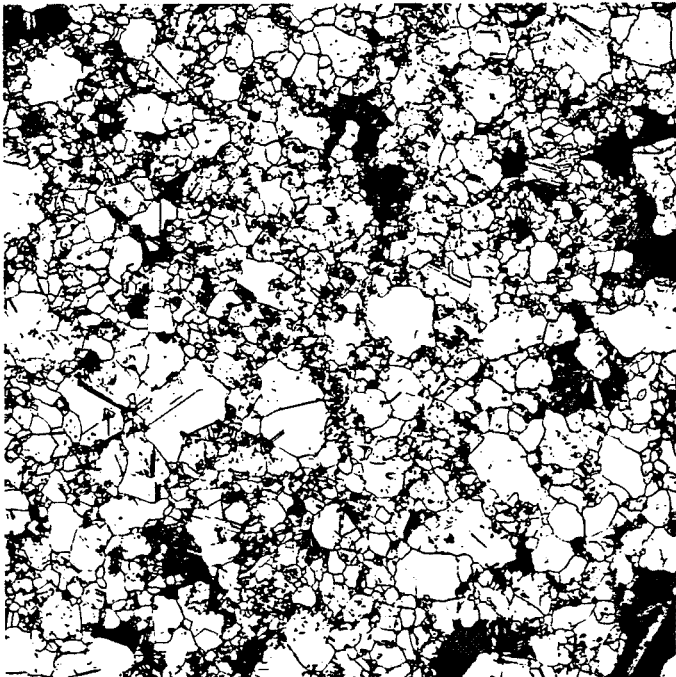see the area between the dotted lines.
50X.
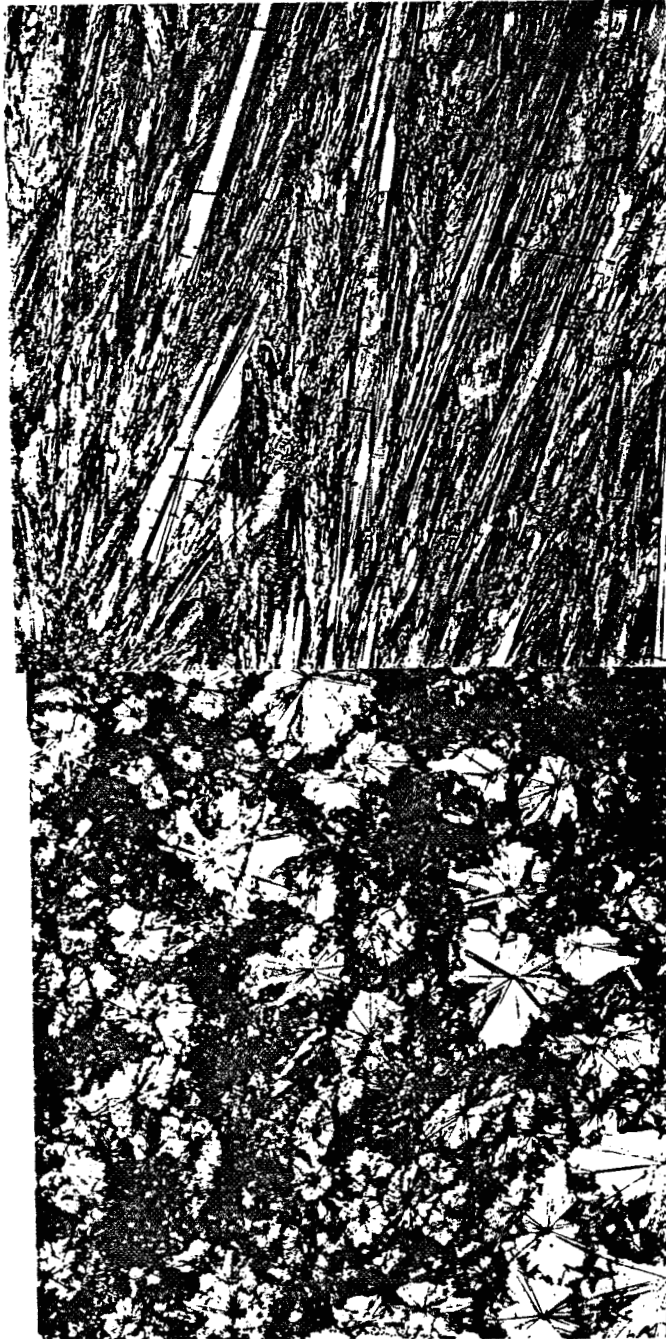
(a)

(b)

Fig.18. (a) shows the grains of as-received
material in a section containing the grain
axes (Face B of figure 16) and (b) shows the
grains in a section perpendicular to their
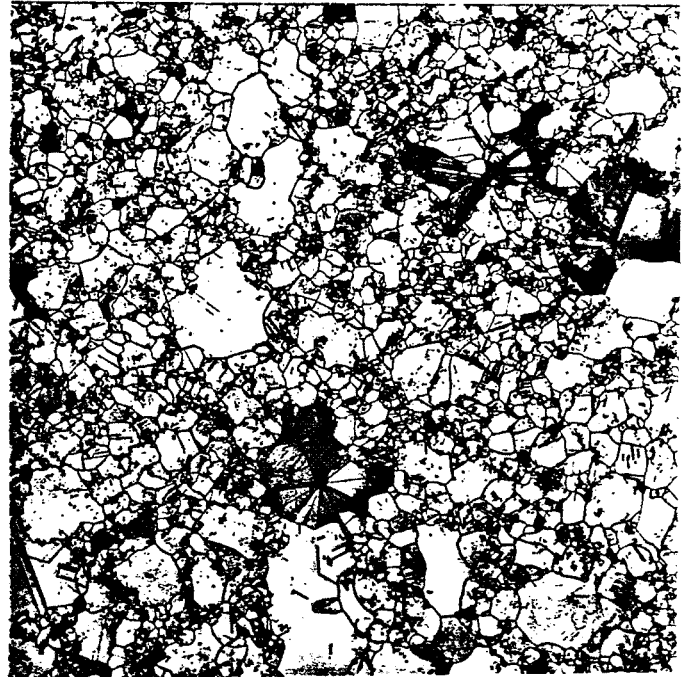axes (Face C of figure 16). 100X

(a)

(b) (c)

Fig. 19.   Sections through a sample annealed
24 hours at 1380°C. (a) is Face B
of figure 16, (b) is Face C near the
center and (c) is Face C near the
platen end. See text for complete
sample history. 100X.

Fig.20. A section through sample P50 after
        compressing 46% at an $\dot{\varepsilon}$ of 5.7 sec^{-1}
        at 1380°C. Some areas recrystallized
        during cooling, see the areas near the
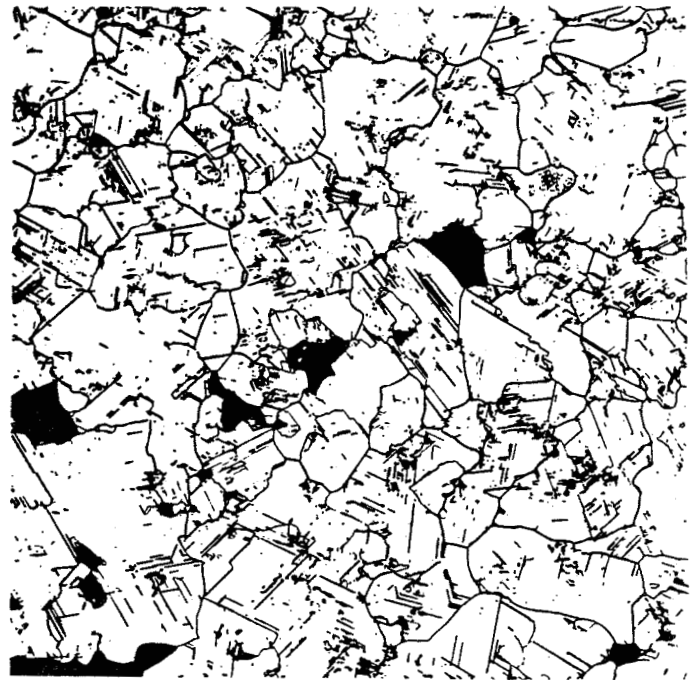   top of the figure. 25X

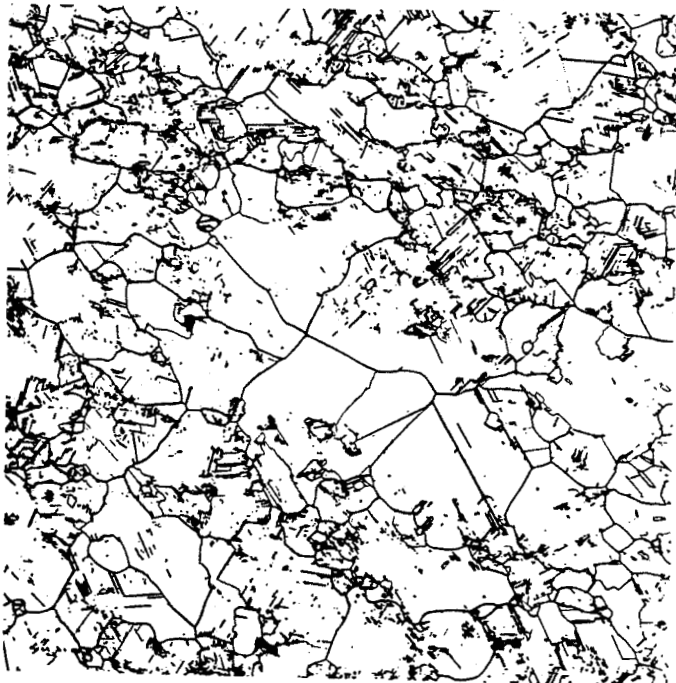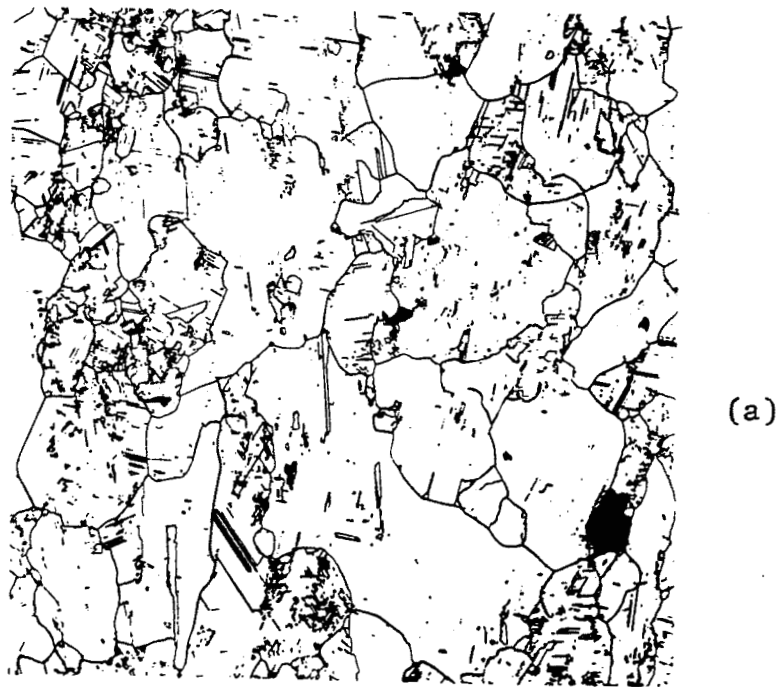(a)

(b)   (c)
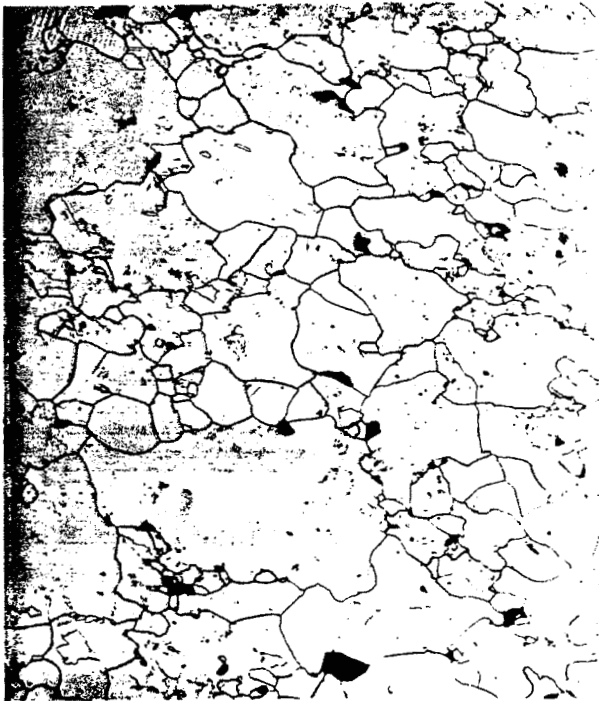
Fig.21.   Sections through sample P53 compressed
          36% at an ε of 4.5 sec^{-1} at 1380°C,
          then annealed for 0.1 hours at 1380°.
          Sequence of sections (a), (b) and (c)
          same as in figure 19.   100X

(a)

(b)   (c)

Fig.22.   As in Figure 21 but annealed 1 hour.
          100X

(a)

(b)   (c)
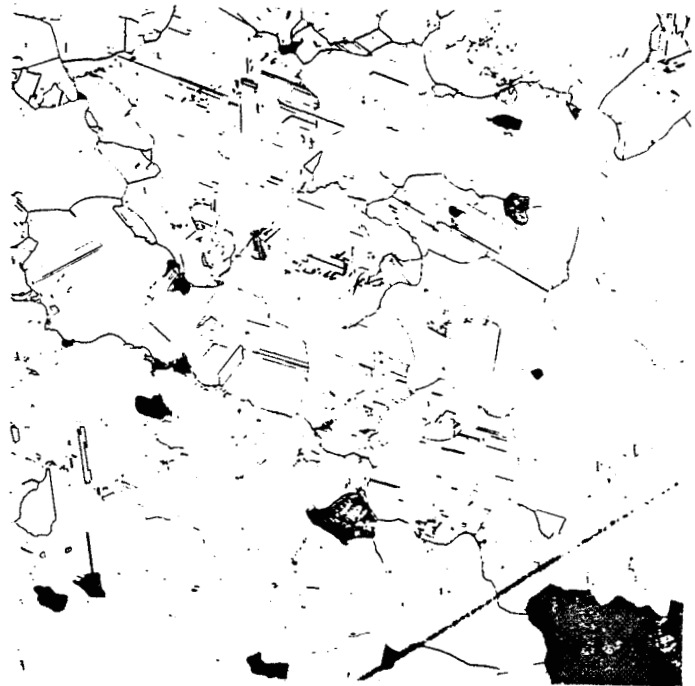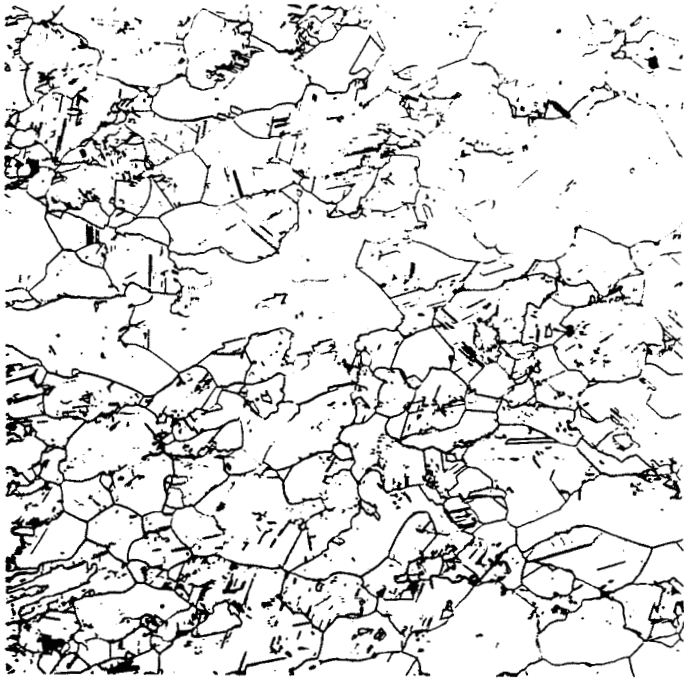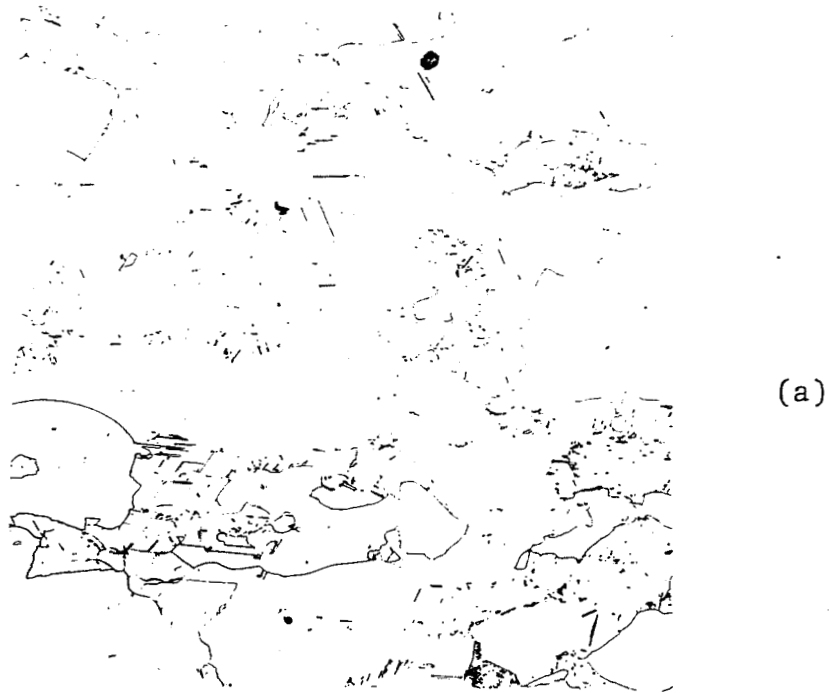
Fig.23.   As in Figure 21 but annealed 10
          hours.   100X

(a)

(b)　　　　　　　　　　(c)

Fig. 24. Sections sample P54 annealed 10 hours
at 1380°C after deformation of 42% at
an $\dot{\varepsilon}$ of 8.5 sec^{-1} at 1376°C, then sub-
mitted to JPL. Section sequence identi-
cal to Figure 19. 100X (continued next
page)

(d)

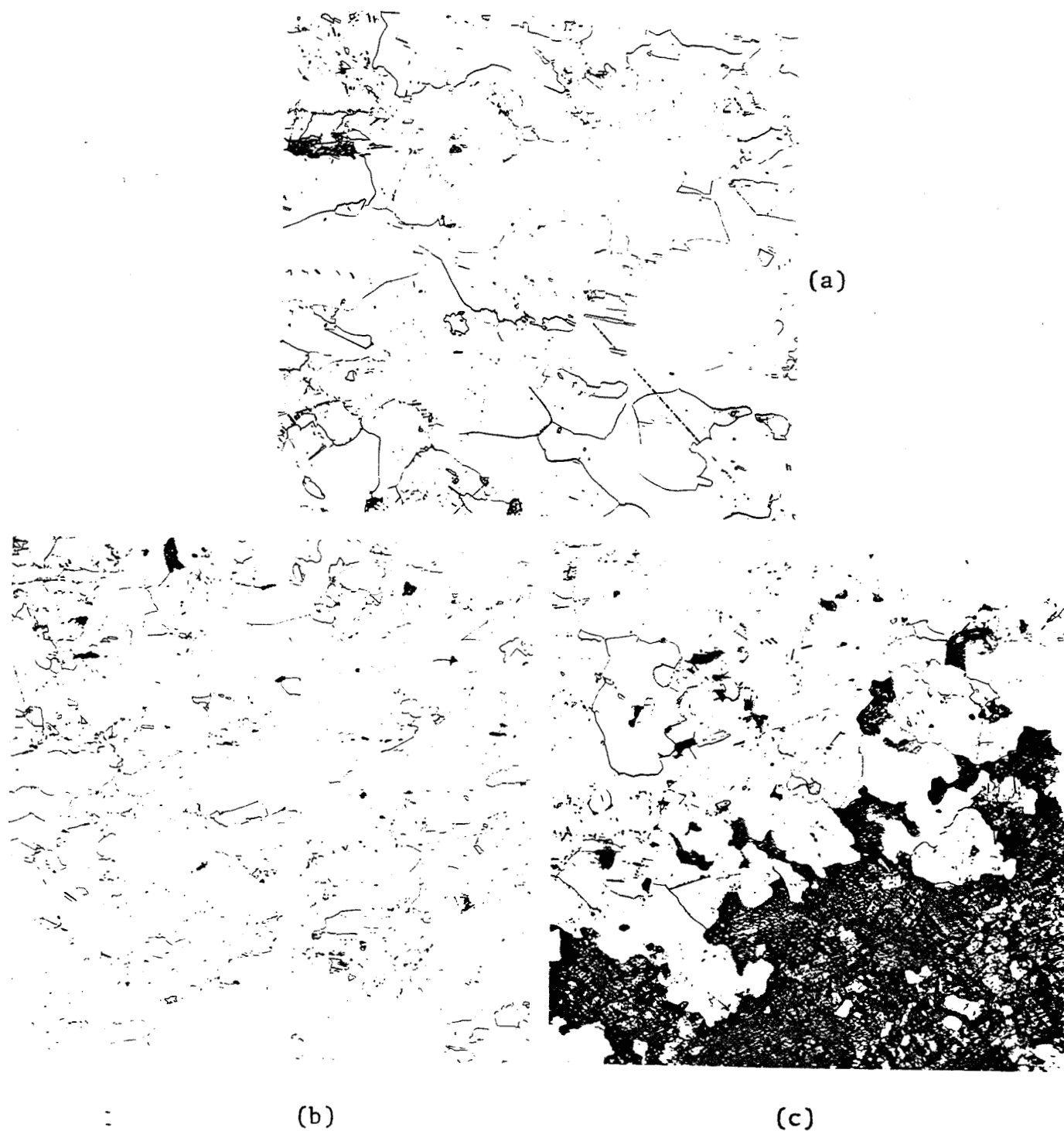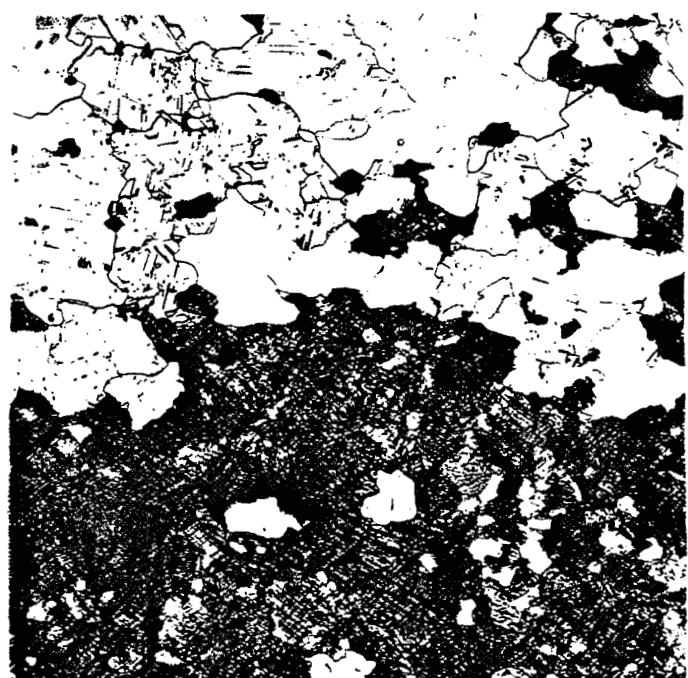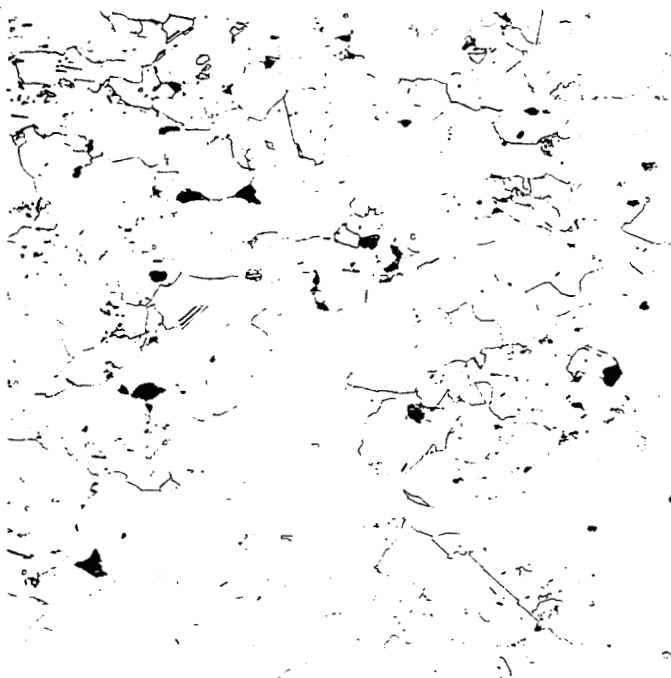(e)   (f)

Fig.24 (cont.). Sections of sample P56 annealed
10 hours at 1380°C after de-
formation of 30% at an $\dot{\varepsilon}$ of
6.1 sec^{-1} at 1380°C, then sub-
mitted to JPL. Section sequence
identical to Figure 19. 100X

Fig.25. An example of partial recrystallization
         due to strain gradients. The light area
         is not recrystallized since plastic flow
         there was restricted by friction on the
         platen. The dark areas are recrystallized.

jpl ⟶

JET PROPULSION LABORATORY *California Institute of Technology • 4800 Oak Grove Drive, Pasadena, California 91103*

September 26, 1977
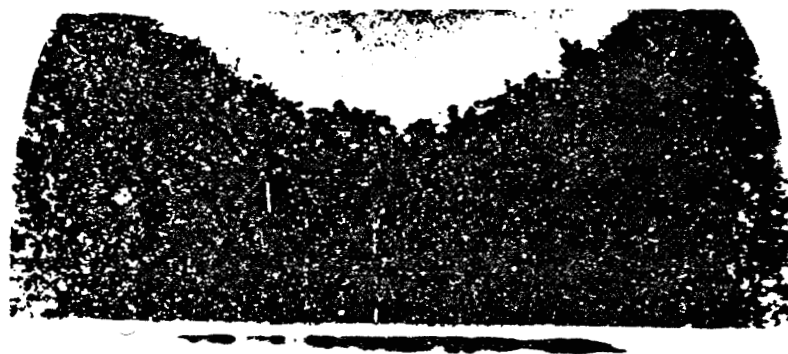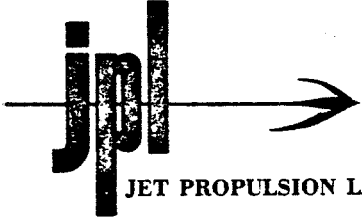
Refer to: 341-TGD:sjt

Dr. Dave Pope
Dr. Chad Graham
University of Pennsylvania
LRSM Bldg.
3231 Walnut
Philadelphia, PA 19104

Dear Dave and Chad:

The following report on diffusion lengths in high temperature uniaxial compressed silicon from the University of Pennsylvania was prepared by Dr. Gary Turner.

The previous letter to Dr. Dave Pope described minority carrier diffusion length (L_n) measurements on p-type silicon samples that had grown polycrystalline (0.2 mm grains) during a Czochralski pull at JPL. Several samples were then subjected to various hot pressing and annealing cycles. All the heat-treated samples suffered a degradation in diffusion length from the original 90 µm to values near zero, but contamination from the apparatus or a too-rapid cooling rate may have been responsible.

Fifteen additional samples have now been measured--a group of six single crystal p-type pieces supplied by JPL and a group of nine p-type poly-crystalline pieces from Dow Corning.

A pair of single crystal samples, P5 and P6, were not heat treated. They both had L_n's of about 30 µm--only fair for single crystal silicon. These were the only ones of the fifteen samples with L_n greater than zero (within the accuracy of the measurement).

Another pair of single crystal samples, P1 and P2, were etched for 3 minutes in 5:3:3 nitric: hydrofluoric : acetic acid, rinsed in DI water, placed in the deformation rig under light preload conditions, and heated at 1380°C for 30 minutes. The surface photovoltage (SPV) signal was fairly strong and reproducible but the flux vs. α^{-1} plot wasn't very linear. Deleting points at short and long wavelengths that curved away from the linear region gave a best guess value of zero.

JET PROPULSION LABORATORY *California Institute of Technology • 4800 Oak Grove Drive, Pasadena, California 91103*

Dr. Dave Pope
Dr. Chad Graham   -2-   Sept. 26, 1977

The third pair of single crystal samples, P7 and P8, were etched, compressed at 1353°C to a total true strain of 0.4 at an average strain rate of 5 sec^{-1} and then annealed at 1380°C for 10 hours. Although the SPV was fairly weak, one of the pair yielded a fairly good straight line indicating zero L_n. (The other had only 4 linear points.)

Since only the untreated samples had nonzero L_n, these data don't show how much degradation is caused by deformation. The nine polycrystalline samples included a pair (P40 and P41) that were heated in quartz ampoules at 1380°C but not deformed. These might have indicated whether the heating-cooling rates alone cause degradation. Unfortunately, even an untreated polycrystal-line sample (P47) had zero L_n. The long anneal of P40 and P41 (24 hrs) might have caused contamination anyway, despite the quartz ampoules.

Notes on the Data:

The quality of the measurement varies widely from sample to sample and several columns of data are included merely to help in judging the quality. Entries in these columns which imply a questionable result are circled for emphasis.

When a sample is mounted in the SPV rig, the first step is to select a signal strength which can be maintained at all wavelengths. This strength, which is kept constant throughout the run, is determined by surface conditions as well as bulk properties, so low signal doesn't always mean short L_n. Low signal does mean low signal noise ratio, though, so large signals are more trustworthy.

The photon flux needed to achieve this signal level is recorded first at the shortest wavelength and then at 12 longer wavelengths. The flux at short wavelength is then remeasured and used to calculate percent "drift". This is a crude measure of quality—a drift of greater than 5% is pretty bad—but shouldn't be taken too seriously since even a very erratic sample may happen to show zero "drift".

When points are plotted on a flux vs. absorption depth (α^{-1}) plot, a straight line should result. Often, however, the plot curves away at short and/or long wavelengths for unknown reasons. Only points in the "straight line region" are used to calculate a least squares straight line fit and the number of points "usable" is a measure of quality—and of the experimenter's prejudice.

The intercept of the straight line is $-L_n$, the diffusion length in μm. The one-sigma standard deviation, S_{bo}, of the fit is also recorded. Note that this only includes statistical error, not systematic, and that statistically

JET PROPULSION LABORATORY *California Institute of Technology • 4800 Oak Grove Drive, Pasadena, California 91103*

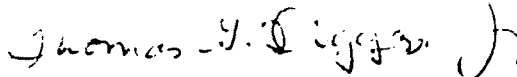Dr. Dave Pope
Dr. Chad Graham   -3-   Sept. 26, 1977

there is a 66% chance of being outside the one-sigma points (but only 2% of being outside three-sigma). The number of points used must also be considered here. After all, if only two points were used, an S_{bo} of zero would be guaranteed.

Sincerely,

Thomas G. Digges, Jr.

cc: M. Larson
     B. Anspaugh

DIFFUSION LENGTH DATA ON SILICON HEAT TREATED BY UNIV. OF PENN.

Sample	Singl/Poly	1st Anneal Temp(°c)/Time(h)	Compression Temp(°c)/Strain/Rate(sec⁻¹)	2nd Anneal Temp(°c)/Time(h)	L_n(μm)	S_{60}(μm)	points	drift(%)	Signal	Note
P 5	S	—	—	—	34	3	11	2.5	1.1 mV	
P 6	S	—	—	—	30	5	(5)	(8.1)	300 μV	1
P 1	S	1380/0.5 preload	—	—	0.8	1.0	(5)	0	300 μV	
P 2	S	1380/0.5 preload	—	—	-0.6	1.5	6	4.7	370 μV	
P 7	S	—	1353 / 0.37 / 5.0	1380 / 10	0.9	0.6	8	2.6	21 μV	
P 8	S	—	1353 / 0.38 / 5.1	1380 / 10	7.4	0.8	(4)	1.8	60 μV	
P 46	P	—	—	—	—	—	0	(13.3)	(0.4 μV)	2
P 47	P	—	—	—	0.2	2.6	9	3.8	16 μV	
P 40	P	1380/24 ampoule	—	—	0.9	1.5	8	4.2	13 μV	
P 41	P	1380/24 ampoule	—	—	1.7	1.2	8	3.0	(1 μV)	3
P 43	P	1380/24 ampoule	—	1380/0.5 preload	3.4	1.3	(4)	0	9 μV	
P 45	P	1380/24 ampoule	—	1380/0.5 preload	3.9	1.3	8	(6.4)	(1 μV)	3
P 51	P	—	1325 / 0.401 / 5.7	—	0.4	1.3	(5)	1.6	3 μV	
P 54	P	1380/24	1376 / 0.42 / 8.5	1380 / 10	-1.2	0.6	8	3.5	6 μV	
P 56	P	1380/24	1380 / 0.30 / 6.1	1380 / 10	0.4	1.3	(5)	0	19 μV	

Notes:
1. Sample has hazy surface, even after repeated etching.
2. Signal very weak and erratic -- too scattered to fit.
3. Signal very weak and erratic. Continuous curve with no part very straight